

AC ELECTRICAL PROPERTIES OF PLASMA POLYMERIZED
1-BENZYL-2-METHYLIMIDAZOLE THIN FILMS

A thesis submitted to the Department of Physics of
Bangladesh University of Engineering and Technology (BUET)
in partial fulfillment of the requirement for the degree of
MASTER OF PHILOSOPHY (M. Phil.) IN PHYSICS

By
Md. Masud Reza
Roll No. 040414034 P
Session : April 2004



DEPARTMENT OF PHYSICS
BANGLADESH UNIVERSITY OF ENGINEERING AND TECHNOLOGY (BUET)
DHAKA-1000, BANGLADESH
SEPTEMBER 2009

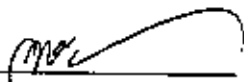
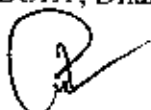
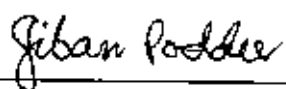
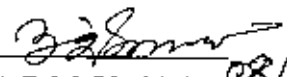
BANGLADESH UNIVERSITY OF ENGINEERING AND TECHNOLOGY, DHAKA
DEPARTMENT OF PHYSICS



Certification of Thesis

The thesis titled "AC ELECTRICAL PROPERTIES OF PLASMA POLYMERIZED 1-BENZYL-2-METHYLIMIDAZOLE THIN FILMS" submitted by Md. Masud Reza, Roll No. 040414034 P. Session: April 2004 has been accepted as satisfactory in partial fulfillment of the requirement for the degree of Master of Philosophy in Physics on 08 September, 2009.

Board of Examiners

1. 
Dr. Md. Abu Hashan Bhuiyan (Supervisor) Chairman
Professor,
Department of Physics
BUET, Dhaka-1000
2. 
Head Member
Department of Physics (Ex-Officio)
BUET, Dhaka-1000
3. 
Dr. Jiban Podder Member
Professor
Department of Physics
BUET, Dhaka-1000
4. 
Dr. A.B.M Obaidul Islam Member
Professor (External)
Department of Physics
University of Dhaka
Dhaka-1000

Candidate's Declaration

It is hereby declared that this thesis or any part of it has not been submitted elsewhere for the award of any degree or diploma.

Signature of the candidate


_____ 08.09.09

(Md. Masud Reza)
Roll No. 040414034 P
Session: April 2004

CONTENTS

Declaration	i
Dedication	ii
List of Figures	vi
List of Tables	viii
Abbreviations and Symbols	ix
Acknowledgements	x
Abstract	xii
CHAPTER I Introduction	
1.1 Introduction	1
1.2 Review of Earlier Research Work	2
1.3 Aim of the Present Study	8
1.4 The Thesis – at a Glance	9
References	9
CHAPTER II Fundamental Concepts of Polymer, Plasma and Plasma Polymerization	
2.1 Introduction	14
2.2 Polymers	14
2.2.1 Physical Properties of Polymers	15
2.2.2 Classification of Polymers	15
2.2.3 Application of Polymers	17
2.3 Polymerization	17
2.4 Different Polymerization Processes	18
2.4.1 Chemical or conventional polymerization processes	18
2.4.2 Physical processes for polymer thin film deposition	19
2.5 Plasma and Plasma Polymerization	19
2.5.1 Plasma	19
2.5.2 Fundamentals of glow discharge processes	22
2.5.3 Direct current (dc) glow discharge	23
2.5.4 Alternating current (ac) glow discharge	23

2.5.5	Plasma polymerization	24
2.6	Different types of Reactors	26
2.7	Advantages and Disadvantages of Plasma Polymers	29
2.8	Applications of Plasma-polymerized Organic Thin Films	29
	References	30

CHAPTER III Experimental Details

3.1	Introduction	33
3.2	The Monomer	33
3.3	Substrate and its Cleaning Process	34
3.4	Capacitively Coupled Plasma Polymerization Set-up	34
3.5	Generation of Glow Discharge Plasma in the Laboratory	37
3.6	Plasma Polymer Thin Film Deposition	38
3.7	Measurement of Thickness of Thin Films	39
3.7.1	Multiple-beam interferometry	39
3.8	Samples for Different Measurements	41
	Reference	41

CHAPTER IV Structural Analyses of PPBMI Thin Films

4.1	Introduction	42
4.2	The Scanning Electron Microscope (SEM)	42
4.2.1	Working Principle of SEM	43
4.2.2	Sample Preparation	44
4.2.3	Experimental Details	44
4.2.4	Results and Discussion	45
4.3	Fourier Transform Infrared Spectroscopy	46
4.3.1	Typical Apparatus	48
4.3.2	Experimental Procedure	49
4.3.3	Results and Discussion	49
	References	51

CHAPTER V Ultraviolet-Visible Spectroscopy of PPBMI Thin Films

5.1	Introduction	53
5.2	Ultraviolet-visible (UV-Vis) Spectroscopy	53
5.2.1	The Electromagnetic Spectrum	53
5.2.2	Electronic Transitions	54
5.3	The Absorption Law	53
5.3.1	Beer-Lambert Law	57
5.4	Instrumentation - Ultraviolet-visible spectrophotometer	58
5.5	Results and Discussion	60
	References	64

CHAPTER VI AC Electrical Properties of PPBMI Thin Films

6.1	Introduction	65
6.2	Theory of Dielectrics	65
6.2.1	Brief Description of dielectrics	65
6.2.2	The Debye theory of dielectrics	67
6.4	Experimental Details	69
6.5	Results and Discussion	71
	References	78

CHAPTER VII Conclusions

7.1	Conclusions	79
7.2	Suggestions for Further Work	80
	Appendix	81

List of Figures

2.1 Structure of linear, branched and crosslinked polymers.....	16
2.2. Different states of water molecules.....	20
2.3. The plasma systems of typical density and temperature conditions.....	21
2.4 Typical setup of Glow Discharge System.....	22
2.5 Comparison of the structures of plasma polymers and conventional polymers.	25
2.6 Formation of polymer with functional group.....	26
2.7 Capacitive Coupling System.....	27
2.8 Inductive Coupling System.....	28
2.9 Electrode less microwavc system.....	28
3.1 Structure of 1-Benzyl-2-Methylimidazole.....	33
3.2 Schematic diagram of the plasma polymerization system.....	34
3.3 Plasma Polymerization system in laboratory.....	36
3.4 Glow discharge plasma during deposition.....	37
3.5 The Schematic diagram of multiple-beam interferometer.....	40
4.1 Schematic diagram of an SEM.....	41
4.2 SEM opened sample chamber.....	44
4.3 Micrographs of PPBMI thin films onto glass substrate	45
4.4 Correlation Table of Infrared Spectroscopy.....	47
4.5 Stretching vibrations	47
4.6 Bending vibrations.....	48
4.7 Typical IR Spectrometer setup.....	48
4.8 The FTIR spectra of BMI and PPBMI thin film.....	50
5.1 Visible part of the Electromagnetic Spectrum.....	54
5.2 Vibration and rotational energy levels of absorbing materials.....	54
5.3 Summery of electronic energy levels.....	55
5.4 Beckman DU640 UV/Vis spectrophotometer.....	59
5.5 Diagram of the components of a typical spectrometer.....	59
5.6 Variation of absorbance, ABS, with wavelength, λ , inset (monomer).....	60
5.7 Absorption co-efficient, α , as a function of photon energy, $h\nu$	61

5.8 $(\alpha h\nu)^2$ versus $h\nu$ curve for PPBMI thin films.....	62
5.9 $(\alpha h\nu)^{1/2}$ versus $h\nu$ curve for PPBMI thin films.....	62
5.10 Plot of extinction co-efficient, k , as a function of $h\nu$	63
6.1 Polarization of dielectrics	66
6.2 Debye dielectric dispersion curves.....	68
6.3 The Edward vacuum coating unit E306A.....	69
6.4 The electrode assembly.....	70
6.5 Photographs of the ac electrical measurement setup.....	71
6.6 Conductivity versus frequency of the PPBMI thin films at	72
6.7 Conductivity versus temperature of the PPBMI thin films at	73
6.8 Dielectric Constant versus frequency of the PPBMI thin films	74
6.9 Dielectric Constant as a function of temperature of the PPBMI thin films.....	75
6.10 Loss Tangent versus frequency of the PPBMI thin films	76
6.11 Loss Tangent as a function of temperature of the PPBMI thin films	77

List of Tables

2.1 Potential applications of plasma-polymerized films.....	29
3.1 General properties of 1-Benzyl-2-Methylimidazole.....	33
4.1 Assignments of FTIR absorption bands for BMI and PPBMI thin film.....	51
5.1 Values of allowed direct and indirect transition energy gaps.....	63
6.1 Values of 'n' at different measurement temperatures of PPBMI thin film.....	72
6.2 Values of 'activation energy' at different frequency of PPBMI thin film.....	73

Abbreviations and symbols used in this thesis

ABS	Absorbance
AC/ac	Alternating Current
Al	Aluminum
B	Tauc Parameter
BMI	1-Benzyl-2-Methylimidazole
Cr-Al	Chromel-Alumel
CC	Capacitively Coupled
d	Sample Thickness
DC/dc	Direct Current
DTA	Differential Thermal Analysis
FL	Fermi Level
FTIR	Fourier Transform Infrared
I	Current
I	Intensity of Radiation
IR	Infrared
J	Current Density
k	Boltzmann Constant
k	Extinction Coefficient
LB	Langmuir-Blodgett
MHz	Mega Hertz
PECVD	Plasma Enhanced Chemical Vapor Deposition
PF	Poole Frenkel
PPBMI	Plasma-Polymerized 1-Benzyl-2-Methylimidazole
PVD	Physical Vapour Deposition
rf	Radio Frequency
SEM	Scanning Electron Microscopy
T _g	Glass Transition Temperature
T _m	Melting Point
Tan δ	Loss tangent
TSDC	Thermally Stimulated Depolarization Current
UV-VIS	Ultraviolet-Visible
V	Voltage
XPS	X-ray Photoelectric Spectroscopy
α	Absorption Coefficient
λ	Wavelength
ΔE	Activation Energy
σ _{ac}	AC Electrical Conductivity
ε'	Dielectric Constant
ε ₀	Permittivity of Free Space
μ	Mobility of the Charge Carrier

Acknowledgements

I express my heartiest gratitude and profound respect to Professor Dr. Md. Abu Hashan Bhuiyan, Department of Physics, Bangladesh University of Engineering and Technology (BUET), Bangladesh for providing the opportunity to work in such a field of study. I am indebted to him for his constant guidance, important suggestions, kind supervision of the research work and also for acquainting me with the world of advance research.

I am grateful to Prof. Dr. Md. Feroz Alam Khan, Head, Department of Physics, BUET for providing all research facilities of the department and for encouraging in completing the work. I am obliged to Prof. Dr. Mominul Huq, Prof. Dr. Nazma Zaman, Prof. Dr. Jiban Podder, Prof. Dr. A.K.M. Akther Hossain, Department of Physics, BUET for their inspiration, affection and constructive suggestions during the progress of research.

I am thankful to Dr. Md. Forhad Mina, Mr. Muhammad Rakibul Islam, Mr. Md. Jellur Rahman, Mr. Md. Samir Ullah, Department of Physics, BUET for their affection and inspiration throughout the work.

I am thankful to the authority of Bangladesh University of Engineering and Technology, BUET, for providing me the financial support.

I am grateful to the Head, Department of Materials and Metallurgical Engineering for permitting me to do SEM. I like to thank Mr. Md. Yousuf Khan, Instrument Engineer, Department of Material and Metallurgical Engineering for helping me to take the SEM.

I am thankful to Dr. M. A. Gafur, Senior Engineer, PP & PDC, and the authority of the Bangladesh Council for Scientific and Industrial Research, Dhaka, for giving me the opportunity to take the FTIR and UV-VIS spectra.

I am grateful to Mr. Mohammad Shoyaib, Assistant Professor, IIT, Dhaka University for helping me to download and print a lot of research papers of this work.

I would like to give special thanks to Ph.D students Mr. Rama Bijoy Sarker, Mr. Sunirmal Mujumder, Mr. Md. Ali Ashraf, Mr. Ahmed Mostofa Kanal, Mrs. Tamanna Afroze, Mrs. Hasina Akther and Mrs. Rummana Matin for their kind cooperation. I want to thank all of my friends who were directly or indirectly related to this work and for giving suggestions.

I like to thank all the staff members of the Department of Physics, BUET specially Mr Md. Idris Munsif, Assistant Technical Officer for their cooperation.

I am grateful to my family members for their love and support to do this research work.

Finally, I am grateful to Almighty Allah for giving me the opportunity to complete the work.

Abstract

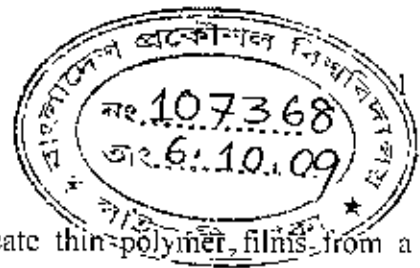
Plasma polymerized 1-Benzyl-2-Methylimidazole (PPBMI) thin films were deposited on to glass substrates by a parallel plate capacitively coupled glow discharge reactor. The PPBMI thin films were characterized by scanning electron microscopy (SEM), Fourier transform infrared (FTIR) spectroscopy, Ultraviolet-Visible (UV-Vis) spectroscopy and ac electrical measurements.

The FTIR spectroscopic analysis indicates that the chemical composition and structure of PPBMI thin films are different from that of 1-Benzyl-2-Methylimidazole (BMI) monomer. The SEM investigation shows a smooth, uniform and pinhole free surface of the PPBMI thin films. The optical properties of PPBMI thin films were investigated by UV-Vis spectroscopy. From the UV-Vis absorption spectra, allowed direct transition (E_{qd}), allowed indirect transition (E_{qi}) energy gaps, Tauc parameter B and extinction coefficient k were determined. The E_{qd} is found to be about 3.00 eV and E_{qi} is about 2.0 eV. The calculated value of Tauc parameter, B , is about $260 \text{ cm}^{-1/2} (\text{eV})^{-1/2}$. The ac conductivity of the films increases with the increase of frequency and temperature. The 'n' values are calculated from ac conductivity versus frequency plots and are found to be about 1.50 to 1.87. The estimated activation energies are calculated and found to be about 0.05 to 0.13 eV for PPBMI thin films. The dielectric constant of PPBMI thin films increases with increasing temperature and slowly decreases in low frequency and rapidly decreases in higher frequency ($>10^4 \text{ Hz}$) ranges. The dielectric constant of PPBMI thin films does not dependent significantly on thickness of the films. The dielectric loss of the thin films increases exponentially with increasing frequency and temperature. The loss peak may occur at the higher frequency and higher temperature.

CHAPTER I

Introduction

- 1.1 Introduction
 - 1.2 Review of Earlier Research Work
 - 1.3 Aim of the Present Study
 - 1.4 The Thesis – at a Glance
- References



1.1 Introduction

Plasma polymerization is a unique technique to fabricate thin-polymer films from a variety of organic and organometallic materials. Plasma polymerized films are pinhole-free and highly crosslinked and therefore are insoluble, thermally stable, chemically inert and mechanically tough. Furthermore such films are often highly coherent and adherent to a variety of substrates including conventional polymer, glass and metal surfaces. Due to these excellent properties they have been undertaken very actively in the last few years for a variety of applications such as per selective membranes, protective coatings, biomedical materials, electronic, optical devices and adhesion promoters [1-12]

Now-a-days thin polymer films find wide applications in microelectronics, coatings for chemical fibers and films, surface hardening of tools, spaceship components and chemical and physical sensors etc. In the thin film technology, plasma polymerization is accepted and is preferred owing to the desirable features of the thin films it yields, because the films produced in plasma have strong adhesion to the substrate surface and pinhole-free character and good optical, electrical, chemical and mechanical properties. It is an elegant technique to produce synthetic diamond from aliphatic hydrocarbons. Polymers frequently replace traditional engineering materials such as metals, glasses and ceramics. The performance of polymers can further be enhanced by applying functional coatings, such as protective layers, optical coatings, gas permeation barriers and others. The desirable bulk properties of polymers are often compromised by unfavorable surface characteristics, such as low hardness, low resistance to abrasion and scratching, and low surface energy that generally leads to poor adhesion [13-16].

Thin polymer films can be formed in two ways: one is wet processing, such as the Langmuir-Blodgett film method, spin-coating, dip-coating and chemical vapor deposition (CVD). Although excellent results have been achieved this way, there are a number of problems that can arise such as pinholes, inclusion of solvents in different polymer layers, contaminants, etc. An alternative approach, which can avoid such difficulties, is plasma polymerization. Among different kinds of polymerization techniques, plasma polymerization emerges as a most important and attractive technique for the preparation of organic thin films. It has been dealt as an extension of polymerization from the academic view point and as a new technology to prepare thin

films from a practical view point. The concept of plasma polymerization has been based on the application of the concept of polymerization and/or of polymers developed in preceding decades to the formation of organic material under plasma conditions. It is possible to modify the surface properties of a substrate, while retaining the transparency and bulk properties of the substrate materials using plasma. Furthermore, it is a solvent-free, fast and versatile process. In the thin film technology, plasma polymerization is accepted and is preferred owing to the desirable features of the thin films it yields, because the films produced in plasma have strong adhesion to the substrate surface and pinhole-free character [14, 16-20].

Research has been performed on several plasma polymerized organic thin films [21-25]. From the literature review, it is seen that the plasma polymerization emerges as a very important technique for thin film deposition and surface modification. The plasma polymerized thin films have also very different physical and chemical properties than their conventionally prepared counterpart. So in the present research work, plasma polymerization technique has been used for organic thin film preparation. On reviewing the earlier works, it is also found that 1-Benzyl-2-Methylimidazole (BMI) has not been used for deposition of plasma polymers. BMI is an aromatic organic compound. The other physical properties will be mentioned in experimental details. These kinds of materials are used as coatings, insulators, dielectrics, etc. That is why this material was chosen as a potential organic monomer for thin film preparation by glow discharge and study of its different properties.

1.2 Review of Earlier Research Work

Plasma polymerization today is gaining recognition as an important process for the formation of entirely new kinds of materials. The materials obtained by plasma polymerization are significantly different from conventional polymers and are also different from most inorganic materials. Thus, plasma polymers lie somewhere between organic polymers and inorganic materials. Plasma polymerization should be considered a method of forming such new types of materials rather than a method of preparing conventional polymers [1]. The structural behavior of plasma polymerized thin films is different than that of the conventionally prepared polymer thin films. Fourier transform infrared (FTIR) spectroscopic analysis, X-ray photoelectron spectroscopy (XPS), X-ray

diffraction (XRD), scanning electron microscopy (SEM), elemental analysis (EA) etc provide information about the chemical structure of the plasma polymers. Ultraviolet visible (UV-Vis) spectroscopic analysis of organic or inorganic materials can provide the information about electronic structure and can ascertain the existence of optical transition mechanisms: allowed direct and indirect transitions and forbidden transitions.

Yifan Xu. and Paul R. Berger [26] deposited Dichlorotetramethyldisiloxane (DCTMDS) films by radio-frequency pulsed plasma polymerization. These films demonstrated very high dielectric constants in the range of 7-10 for a polymer based system. The variation of dielectric constant does not show any trend with varying film thickness, indicating that the thickness of the deposited films is not significant for controlling permittivity. Poly (3-hexythiophene) polymer field effect transistors (PFETs) using PPP DCTMDS gate dielectric films were fabricated. Due to the high dielectric constants of PPP DCTMDS, the PFETs posses high gate capacitance and operate at low voltage. Kim M.-C. et al.[27] reported that thiophene films produced by plasma enhanced chemical vapor deposition method at 373 K have highly oriented amorphous polymer structure. The films also have the same stoichiometric ratio (8:1) between Carbon and Sulfur, indicating that dimmer-like thin films were produced. The relative dielectric constants of the films was increased from 2.96 to 4.0 when the RF power was increased up to 200 W. Moreover, the leakage current density was increased with increasing RF power and deposition temperature. The maximum deposition rate obtained was 110 nm/min for the polymerized thin film deposited at 300 K and 100 W.

Plasma polymerized N, N, 3, 5 Tctramethylaniline (PPTMA) thin films were deposited on to glass substrates at room temperature by a capacitatively coupled parallel plate reactor by Akther H. and Bhuiyan A. H. [28]. The structural analyses have revealed that PPTMA thin films are formed with certain amount of conjugation, which modifies on heat treatment. From the UV-Vis absorption spectra, allowed direct transition (E_{qd}) and indirect transition (E_{qi}) energy gaps are determined to be 2.80 and 1.56 eV respectively, while E_{qd} increases a little, E_{qi} decreases, on heat treatment of PPTMA thin films. The calculated values of Tauc parameter B for all the samples indicate an increase in structural order/conjugation in PPTMA thin films improved by heat treatment. The allowed direct and indirect transition energy gaps are also modified when the samples are

heat treated. Akther H. and Bhuiyan A. H. [29] reported on electrical and optical properties of PPTMA thin films deposited onto glass substrates at room temperature. Elemental analysis, IR and UV-Vis spectroscopy revealed that there are conjugations in the matrix of the PP1MA thin films. From UV-Vis spectroscopy they found that indirect energy gap varies from 1.49 to 1.86 eV with film thickness.

Li K. et al. [30] studied the molecular structure of plasma polymerized organosiloxane thin films. The results of the analysis evidence that the molecular structure of the growing film is not homogeneous. Electron microscopy analysis showed that the deposition in HMDSO low pressure rf plasmas on substrates with a porous surface results in the formation of films with a morphology demonstrating spherical or hemispherical structures. The films deposited in an O₂/HMDSO plasma at the driven electrode show the absorption lines shifted to shorter wavelengths. The intensive HMDSO fragmentation at long plasma-on times results in the growth of dense films with slightly lower content of organic constituent. A mass spectroscopic study of the stable neutral gases products shows that the HMDSO conversion can be controlled by the power input and O₂ admixture. Wrobel et al. [31] analysed the structure of plasma polymerized siloxanes by means of pyrolysis/gas chromatography and mass spectroscopy and found that plasma polymerization of linear siloxanes yields only linear oligomers in the volatile fraction extracted from a film.

Saravanan S. et al. [32] investigated low dielectric constant *k*, thin films based on rf plasma polymerized aniline. They found that capacitance and dielectric loss decrease with increase of frequency and increase with increase of temperature. The films exhibit low dielectric constant values, which are stable over a wide range of frequencies and are probable candidates for low *k* applications. The FTIR studies have revealed that the aromatic ring is retained in the polyaniline, thereby increasing the thermal stability. They measured dielectric constant and ac conductivity in the frequency range 100 Hz – 1 MHz and the temperature range 300 – 373 K. The dielectric permittivity in the high frequency range is considerably low.

Bae I.-S. et al. [33] deposited Methylcyclohexane and ethylcyclohexane plasma polymerized thin films. The films showed high optical transmittance up to 80%. FTIR and UV-VIS results show that the as-grown films have some oriented structures. AFM

data show quite smooth and dense surface morphology with increasing RF power. The optical refractive index of methylcyclohexane polymer films show more higher value than that of ethylcyclohexane films while the contact angles of methylcyclohexane films have relatively lower values than that of ethylcyclohexane films, indicating more high surface energy for the methylcyclohexane films.

Antonio P. et al. [34] study the species and polarity of the surface of oxygenated organic thin films which are used in sensors for environmental control. To produce hydrophilic films, ethanol, acetone and 2-propanol are used. From the experiments, it is showed that ethanol is not a promising reagent to obtain plasma polymerized hydrophilic films. FTIR analysis pointed out CH_n , CH_2 , CH_3 , OH and C=O absorption. The increase in C=O intensity occurs simultaneously with OH decrease, which seems to indicate that C=O was formed at the expense of OH species. The films obtained from 2-propanol and acetone monomers were hydrophilic, and could be wetted by water and organic liquids (2-propanol and acetone). However, acetone films showed contact angles higher than 2-propanol films.

Sajeev U. S. et al. [35] reported the pristine and iodine doped polyaniline thin films prepared by ac and rf plasma polymerization techniques separately for the comparison of their optical and electrical properties. The structural properties of these films were evaluated by FTIR spectroscopy and the optical band gap was estimated from UV-VIS-NIR measurements. They have found the optical band gap of polyaniline thin films prepared by rf and ac plasma polymerization techniques differ considerably and the band gap is further reduced by in situ doping of iodine. The electrical conductivity measurements on these films show a higher value of electrical conductivity in the case of rf plasma polymerized thin films when compared to the ac plasma polymerized films.

Peng He. et al. [36] deposited carbonfluorine thin films of aligned carbon nanotubes using a plasma polymerization treatment. The study of high-resolution transmission electron microscopy images revealed that a thin film of the polymer layer (20 nm) was uniformly deposited on the surfaces of the aligned carbon nanotubes. Time-of-flight secondary ion mass spectroscopy and Fourier transform infrared identified the carbonfluorine thin films on the carbon nanotubes. The coated film will form a highly cross-linked and ring like structure which does not exist in the original monomer.

Meichsner J. and Li K. [37] reported the characterization of thin-film formation in molecular low temperature plasmas. They showed that in low-pressure gas discharge the different plasma species like ions, electrons reactive neutrals and photons interact with the substrate/film surface simultaneously. Due to the interaction of energetic plasma species with solid substrates, the surface may be activated and / or free macroradicals may be formed. These processes result in the enhanced adsorption of incoming particles which may considerably influence chemical surface reactions and thin-film growth.

Cech V. et al. [38] prepared thin plasma polymer films from a mixture of dichloro(methyl)phenylsilane (DCMPS) vapour and gaseous hydrogen. They investigated the mechanical, thermal, optical and electrical properties of the thin films and revealed that the plasma polymer film was amorphous and relatively rigid material at room temperature. The IR spectra revealed a great quantity of oxygen atoms in deposited layers. A decomposition of the material with increasing temperature results in a shift of the luminescence spectra to smaller energies, from blue to yellow light for the case of emission spectra. PDCMPS can be used to construct a single-layer LED with the blue light.

Yifan Xu et al. [39] prepared insulating polymer films of Allylamine at plasma reactor temperatures of 25^o C and 100^o C. Multiple frequency capacitance-voltage (C-V) measurements indicated that an in-situ heat treatment during film deposition increased the insulator dielectric constant. The dielectric constant, calculated from the C-V data, rose from 3.03 for samples with no heat treatment to 3.55 for samples with an in-situ heat treatment. For both sample sets, the I-V data demonstrates a low leakage current value (<20fA) up to 100 V. Capacitance-time (C-t) measurements were also used to characterize the mobile ions in the polymer that migrate over time with applied voltage. Results indicate that the polymer layers contain few electrically active defect centers and virtually no pinholes.

Lefohn Aaron E. et al. [40] prepared thin nitrogen-containing films from both pulsed and CW plasmas using acetonitrile and acrylonitrile monomer. They reported that with acetonitrile, film composition does not change appreciable by varying applied rf power or duty cycle. This is in sharp contrast to the level of control over film chemistry they have achieved with pulsed plasma polymerization of other monomers. Films deposited from

the more complex monomer acrylonitrile, however, do exhibit functional group changes with both applied power in CW plasmas and duty cycle in pulsed plasmas. They suggested that careful and thoughtful selection of starting materials for pulsed plasma polymerization can result in effective molecular tailoring of materials.

Ramm M. et al. [41] studied the polymerization of C_{60} under different Ar plasma conditions. Films were either deposited in the pressure range between 1.3 and 40 Pa applying input power of 50 W or evaporated C_{60} films were exposed to Ar plasma and 50 W. The films were investigated by Raman spectroscopy, XPS and carbon K near-edge X-ray-absorption fine structure spectroscopy (NEXAFS). The films were non-uniform and consisted of unpolymerized C_{60} , dimmers, linear chains and polymeric planes. In comparison with evaporated C_{60} the XPS C 1s peak is broader and asymmetric for the C_{60} polymer and its shake-up satellites diminished. Optical parameters (refractive index, dispersion energy, optical gap) of polymethylmethacrylate (PMMA) layers has been studied by Svoreik V. et al. [42]. They reported that electric field imposed to layers during their preparation increases their refractive index.. dispersion energy E_d increases with decreasing layer thickness, no significant differences in surface morphology and roughness between non- and oriented PMMA layers, sharp increase of light absorption occurs in PMMA under 220 nm which corresponds to $\pi \rightarrow \pi^*$ transitions of $-COOCH_3$ structures, a higher level of order in the material causes higher values of optical gap.

Pradhan Dilip K. et al. [43] studied the effect of plasticizer (PEG₂₀₀) on dielectric and electrical properties of plasticized polymer nanocomposite electrolytes. They reported that at low frequency, the variation of relative dielectric constant with frequency shows the presence of material electrode interface polarization processes. The loss tangent peaks appearing at a characteristic frequency suggest the presence of relaxing dipoles in all the samples. The frequency dependence of ac conductivity follows the universal power law with a small deviation in the low frequency region due to the electrode polarization effect. The conductivity increases with increase in plasticizer concentration. Analysis of electrical modulus and dielectric permittivity functions suggest that ionic and polymer segmental motions are strongly coupled.

Semiconductor-like thin films were grown using metallic phthalocyanines (MPc) (M=Fe, Pb, Co) and 1,8 dihydroxiantraquinone by Sanchez M.E. et al. [44]. The effect of

temperature on conductivity was measured of the films and it was found that the temperature-dependent electric current in all cases showed a semiconductor behavior with conductivities in the order of $10^{-6} \Omega^{-1} \text{cm}^{-1}$. The calculated optical band gap values of these materials as well as the magnitude of their electrical conductivities of the thin films suggest the possibility of considering them for use in the preparation of electronic devices.

1.3 Aim of the Present Study

In the field of materials science and technology, plasma polymerization is an important technique of synthesis, which produces thin films of polymers that differ slightly from conventional polymers in terms of their structure and morphology, but retain the majority of its properties. Most polymers contain some polar groups and the dielectric behaviour of plasma polymerized polymers is a function of frequency, time and temperature. Moreover, detailed studies of dielectric parameters such as the dielectric constant and the dielectric loss tangent ($\tan\delta$) over a wide range of frequencies and temperature can provide some significant information on structural, optical and ac electrical behaviour about these polymers.

There is no report on experimental studies of electrical properties on 1-Benzyl-2-Methylimidazole (BMI) based materials. So BMI was chosen as a potential organic monomer for thin film preparation and study of the structural, optical and ac electrical properties of thin films prepared from BMI by plasma polymerization technique. The aim of the present study is to prepare thin films of BMI by plasma polymerization technique and to characterize those using different physical techniques. Plasma polymerized 1-Benzyl-2-Methylimidazole (PPBMI) thin films are to be deposited at optimized glow discharge condition. The surface structure, the chemical structure, the absorption coefficient, optical energy gaps and ac electrical conduction and dielectric relaxation processes are investigated.

The ac electrical measurements are performed at different frequencies and temperatures on samples of different thicknesses. The observed results are analyzed using existing dielectric theories. This helps to understand the ac conduction behaviour and relaxation properties of the material. These findings add new knowledge in the field of dielectric

properties of plasma polymerized organic thin films, which may indicate some suitable application of this type of material in the electrical and electronic devices.

1.4 The Thesis - at a Glance

This research work has been configured into seven chapters. Chapter one presents a general introduction. Some earlier and a number of literatures of recent works are reviewed to understand the scientific importance of those need for the present investigation and the objectives of the study.

Chapter two describes the details about polymers, plasma polymers, different polymerization processes, advantages and disadvantages of plasma polymers. Application of plasma polymerized organic thin films is presented at the end of this chapter.

The experimental techniques are briefly explained in chapter three along with the description of the plasma polymerization set up, generation of glow discharge, film thickness measurements, sample formation etc. The monomer, substrate materials and its cleaning process are also included here.

In chapter four, the experimental details and results of SEM and FTIR are discussed. The UV-VIS spectroscopic analysis is presented in chapter five. The experimental details of UV-VIS absorption measurement and calculated values of direct and indirect transition energy gaps are discussed here.

Chapter six begins with a brief account of the theories on ac conductivity. The ac properties such as variation of ac conductivity, dielectric constant, dielectric loss tangent with frequency and temperature are presented to characterize the PPBM1 thin films.

Finally the conclusions of the work done and suggestions for future research on this material are included in chapter seven.

References

- [1] Yasuda H., Plasma Polymerization, Academic Press, NY (1985).
- [2] Hinman P.V., Bell A.T. and Shen M., "Composite reverse osmosis membranes prepared by plasma", J. Appl. Polym. Sci. 23 (1979) 3651.
- [3] Cho D.L. and Yamada H., Proceedings of the ACS Division of Polymeric Material 57 (1987) 599.
- [4] Yasuda H. and Gazicki M., Biomaterials 3 (1982) 68.

- [5] Hollahan R. and Bell A.T., "Techniques and applications of plasma chemistry". John Wiley and Sons (1984).
- [6] Hatori S., "Vacuum lithography using plasma polymerization and plasma development", *Thin Solid Films* 83 (1981) 189-194.
- [7] Morita S. and Hatori S., *Application of plasma polymer, plasma deposition, treatment and etching of polymer*, edited by R. D'Agostino, Academic Press, Boston (1990).
- [8] Osada Y., Mizumoto A. and Tsuruta H., "Photovoltaic and catalytic activity of plasma polymerized. phthalocyanine films", *J. Macromol. Sci. Chem.* A24 (1987) 403-418.
- [9] Tien P.K., Smolinski G. and Martin R.J., "Thin organosilicon films for integrated optics", *Appl. Optics* 11(3) (1972) 637.
- [10] Biederman H. and Osada H., *Plasma Chemistry of Polymers*, (1989) 57 – 109
- [11] Moshonov A., Avni Y., *J. Appl. Polym. Sci.* 25 (1980) 771.
- [12] Inagaki N. and Yasuda H., "Adhesion of glow discharge polymers to metals and polymers", *J. Appl. Polym. Sci.* 26 3333.
- [13] Fang J., Chen H. and Yu X., "Studies on plasma polymerization of hexamethyldisiloxane in the presence of different carrier gases", *J. Appl. Polym. Sci.* 88 (2001) 1434-1438.
- [14] Moser E.M., Faller Ch., Pietrzko S. and Eggimann F., "Modeling the functional performance of plasma polymerized thin films", *Thin Solid Films* 355-356 (1999) 49-54.
- [15] Shi Frank F., "Developments in plasma-polymerized organic thin films with novel mechanical, electrical, and optical properties", *J. M. S. Rev. Macro Chem. Phys.* 36(4) (1996) 795-826.
- [16] Inagaki N., Tasaka S. and Hiramatsu H., "Preparation of oxygen gas barrier poly(ethylene terephthalate) films by deposition of silicon oxide films plasma polymerized from a mixture of methoxysilane and oxygen.", *J. Appl. Polym. Sci.* 71 (1999) 2091-2100.
- [17] Bell A.T. and Shen M. (Eds.), "Plasma Polymerization", Am. Chem. Soc. Washington, DC (1979).

- [18] Suhr H. and Bell A.T., "Techniques and applications of plasma chemistry". Hollahan, Ed., John Wiley & Sons: NY (1974) 57-111.
- [19] Fang J., Chen H., Yu X., "Studies on plasma polymerization of Hexamethyldisiloxane in the presence of different carrier gases", *J. Appl. Polym. Sci.* 88 (2001) 1434-1438.
- [20] Dahl S., Rats D., Martinu L., Klemberg-Sapieha J.E. "Micromechanical characterization of plasma treated polymer surface", *Thin Solid Films* 355-356 (1999) 290-294.
- [21] Mustari Zaman, "Preparation and study of DC electrical mechanism in plasma polymerized thin films of tetrachlorosilicate", M.Phil. Thesis, BUET, Dhaka (2005).
- [22] Akther H., "Preparation and study of the electrical properties of plasma polymerized thin films N,N,3,5 tetramethylaniline", M.Phil. Thesis, BUET, Dhaka (2004).
- [23] Chowdhury F.-U.-Z., "Preparation and characterization of plasma polymerized diphenyl thin films", Ph.D. Thesis, BUET, Dhaka (2000).
- [24] Md. Rezaul Karim, "Preparation and Investigation of the optical and DC electrical properties of plasma polymerized thin films of 1,1,3,3 Tetramethoxypropane", M.Phil. Thesis, BUET, Dhaka (2005).
- [25] Tamanna Afroze, "Investigation of the dielectric relaxation in plasma polymerized 1,1,3,3 Tetramethoxypropane thin films", M.Phil. Thesis, BUET, Dhaka (2007).
- [26] Yifan Xu, and Paul R. Berger; "Pulsed plasma polymerized dichlorotetramethyldisiloxane high - k gate dielectric for polymer field effect transistors", *J. Appl. Phys.* 99 (2006) 014104.
- [27] Kim M.-C., Cho S. -H., Lee S. -B., Kim Y., Boo J. -H., "Characterization of polymer - like thin films deposited on silicon and glass substrates using PECVD method", *Thin Solid Films* 447-448 (2004) 592-598.
- [28] Akther H. and Bhuiyan A. H., "Infrared and ultraviolet-visible spectroscopic investigation of plasma polymerized N,N,3,5 tetramethylaniline thin films". *Thin Solid Films* 474 (2005) 14-18.

- [29] Akther H. and Bhuiyan A. H., "Electrical and optical properties of plasma polymerized N,N 3, 5 tetramethylamine thin films". *New J. Phys.* 7 (2005) 173.
- [30] Li K., Gabriel O. and Meichsner J., " Fourier transform infrared spectroscopy study of molecular structure formation in thin film during hexamethyldisiloxane decomposition in low pressure rf discharge", *J. Phys. D:Appl. Phys.* 37 (2004) 588-594.
- [31] Wrobel A. M., Kryszewski M., Gazicki M., "Oligomeric products in plasma polymerized organosilicones", *J. Macromol. Sci., Part A: Pure and Appl. Chem.* 1520-5738 20 5 (1983) 583-618.
- [32] Saravanan S., Joseph Mathai C., Venkatachalam S., "Low k thin films based on rf plasma-polymerized aniline", *New J. Phys.* 6 (2004) 64.
- [33] Bae I.-S., Cho S. -H., Lee S.-B., Kim Y., Boo J.-H., "Growth of plasma-polymerized thin films by PECVD method and study on their surface and optical characteristics", *Surf. Coat. Tech.* 193 (2005) 142-146.
- [34] Antonio P. Nascimento Filho, Maria L. P. Silva, "Polymer production by plasma polymerization of oxygenated organic compounds". *Polimers* 12 4 (2002).
- [35] Sajeev U. S., Joseph Mathai C., Saravanan S., Venkatachalam S. and Anantharaman M. R., "On the optical and electrical properties of rf and ac plasma polymerized aniline thin films", *Bull. Mater. Sci.* 29 2 (2006) 159-163.
- [36] Peng He, Donglu Shi, Lian Jie, Wang L. M., Li W. Z., Ren Z. F., "Plasma deposition of thin carbonfluorine films on aligned carbon nanotube", *Appl. Phys. Lett.* 86 (2005) 043107.
- [37] Meichsner J., Li K., "In situ characterization of thin-film formation in molecular low-temperature plasmas", *Appl. Phys. A* 72 (2001) 565-571.
- [38] Cech V., Horvath P., Jancar J., Schauer F., Nespurek S., "Plasma-polymerized DCMPS as adhesive film", *Chem. Papers* 53 3 (1999) 165-173.
- [39] Yifan Xu, Paul R. Berger, Jai Cho and Richard B. Timmons, "Capacitance-voltage characterization of pulsed plasma polymerized allylamine dielectrics for flexible polymeric field effect transistors", *J. Elec. Materials* 33 (2004) 10.

- [40] Lefohn Aaron E., Mackie Neil M. and Fisher R., "Comparison of films deposited from pulsed and continuous wave acetonitrile and acrylonitrile plasmas", *Plasmas and Polymers* 3 (1998) 4.
- [41] Ramm M., Ata M., Gross Th. and Unger W., "Plasma-polymerized C₆₀ films", *Mater. Phys. Mech.* 4 (2001) 8-12.
- [42] Svoreik V., Lyutakov O., Huttel I., "Thickness dependence of refractive index and optical gap of PMMA layers prepared under electrical field", *J. Mater Sci: Mater Elec.* 19 (2008) 363-367.
- [43] Pradhan Dilip K., Choudhary R. N. P., Samantaray B.K., "Studies of dielectric relaxation and ac conductivity behavior of plasticized polymer nanocomposite electrolytes", *Int. J. Electrochem. Sci.* 3 (2008) 507-608.
- [44] Sanchez Vergara M.E., Ortiz Rebollo A., Alvarez J.R., Rivera M., "Molecular materials derived from MPc (M = Fe, Pb, Co) and 1, 8-dihydroxiantraquinone thin films: formation, electrical and optical properties", *J. Phys. and Chem. Solids* 69 (2008) 1-7.

Chapter II

Fundamental Concepts of Polymer, Plasma and Plasma Polymerization

- 2.1 Introduction
 - 2.2 Polymers
 - 2.2.1 Physical Properties of Polymers
 - 2.2.2 Classification of Polymers
 - 2.2.3 Application of Polymers
 - 2.3 Polymerization
 - 2.4 Different Polymerization Processes
 - 2.4.1 Chemical process or conventional polymerization processes
 - 2.4.2 Physical processes for polymer thin film deposition
 - 2.5 Plasma and Plasma Polymerization
 - 2.5.1 Plasma
 - 2.5.2 Fundamentals of glow discharge processes
 - 2.5.3 Direct current (dc) glow discharge
 - 2.5.4 Alternating current (ac) glow discharge
 - 2.5.5 Plasma polymerization
 - 2.6 Different types of Reactors
 - 2.7 Advantages and Disadvantages of Plasma Polymers
 - 2.8 Applications of Plasma-polymerized Organic Thin Films
- References

2.1 Introduction

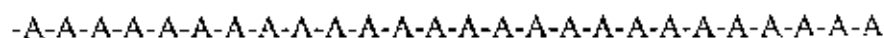
Polymeric materials have a vast potential for exciting new applications in the foreseeable future. Polymer uses are being developed in diverse areas such as: conduction and storage of electricity, molecular based information storage and processing, molecular composites, unique separation membranes, new forms of food processing and packaging, health, housing and transportation. Indeed, polymers will play an increasingly important role in all aspects of everyday life. The large number of current and future applications of polymeric materials has created a great interest for scientists to carry out research and development in polymer science and engineering [1].

This chapter presents a detail of polymers and their general properties and different-polymerization processes. The details of plasma, an overview of gas discharge plasma, plasma polymerization, different types of glow discharge reactors, plasma polymerization mechanism, advantages and disadvantages of plasma polymerized thin films are illustrated in this chapter. Application of plasma polymerized organic thin films is focused at the end of the chapter.

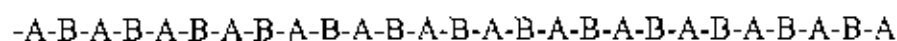
2.2 Polymers [2-4]

Polymers are a very important class of materials. Polymers in the natural world have been around since the beginning of time. Starch, cellulose and rubber all possess polymeric properties. Man-made polymers have been studied since 1832. Today, the polymer industry has grown than the aluminum, copper and steel industries combined.

Polymers are long chain giant organic molecules are assembled from many smaller molecules called monomers. Polymers consist of many repeating monomer units in long chains. A polymer is analogous to a necklace made from many small beads (monomers). Let us imagine that a monomer can be represented by the letter A. Then a polymer made of that monomer would have the structure:



In another kind of polymer, two different monomers might be involved. If the letters A and B represent those monomers, then the polymer could be represented as:



A polymer with two different monomers is known as a copolymer.

2.2.1 Physical Properties of Polymers

The properties of polymers are dependent on many factors including inter and intra chain bonding, the nature of the backbone, processing events, presence or absence of additives including other polymers, chain size and geometry, and molecular weight distribution. While most materials have melting or freezing and boiling or condensing points, polymers do not boil because the energy necessary to put a polymer into the vapor state is greater than the bond energies of the atoms that hold the polymer together, thus they degrade prior to boiling [5].

2.2.2 Classification of Polymers [3, 5-14]

There are many ways in which polymer properties or behaviors are classified to make general descriptions and understanding.

Classification based upon the physical property related to heating

Thermoplastics are materials, which can be heated and formed, then re-heated and re-formed repeatedly. Examples: Polystyrene, Polyethylene, Recyclable food containers etc.

Thermoset materials undergo a chemical as well as a phase change when they are heated. Their molecules form a three-dimension cross-linked network. Example: Phenol-formaldehyde resins, Melamine paints, Permanent adhesives, Coatings etc.

Classification based upon the reaction mode of polymerization

Addition Polymers are the monomer molecules bond to each other without the loss of any other atoms. Example: Ethylene polymerization to generate poly(ethylene).

Condensation Polymers are usually two different monomers combine with the loss of a small molecule, usually water. Polyesters and polyamides (nylon) are in this class of polymers.

Classification based upon the chemical microstructure

Homopolymers are polymers derived from a single monomer (can be linear, branched or crosslinked). Example: Poly(ethylene), Poly(butadiene).

Random Copolymers are two monomers randomly distributed in chain. Example: Poly(acrylonitrile-ran-butadiene)

Alternating Copolymers are two monomers incorporated distributed sequentially. Example: Poly(styrene-alt-maleic anhydride)

Block Copolymers are linear arrangement of blocks of high molecular weight. Example:

Poly(styrene-*b*-butadiene-*b*-styrene)

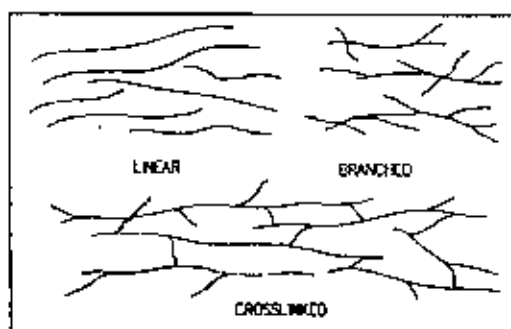
Graft Copolymers are differing backbone and side-chain monomers. Example:

Poly(isobutylene-graft-butadiene)

Classification based upon the Chain Architecture

Linear polymers are one without branches.

Branched polymers are one with an appreciable number of side-chains are classified as branched. These side chains may differ in composition from the polymer backbone.



2.1 Structure of linear, branched and crosslinked polymers

Crosslinked polymers have a continuous network of polymer chains.

Classification based upon the Crystallinity

Crystalline polymers are nearly linear structure, which have simple backbones. tend to be flexible and fold up to form very tightly packed and ordered crystalline areas.

Amorphous polymers are bulkier molecular chains or large branches or functional groups tend to be stiffer and will not fold up tight enough to form crystals.

Polymers can also be classified as:

- a) Natural Polymers
- b) Synthetic Polymers

Natural polymers are very common in nature; some of the most widespread naturally occurring substances are polymers. Starch and cellulose are examples.

Synthetic polymers are produced commercially on a very large scale and have a wide range of properties and uses. The materials commonly called plastics are all synthetic

polymers. Different types of Synthetic polymers are elastomers, thermosets, thermoplastics, fibers, plastics, coatings, films, composites etc.

2.2.3 Applications of Polymers [2]

Some common applications of the polymer are in:

Agriculture and Agribusiness

- Polymeric materials are used in and on soil to improve aeration, provide mulch, and promote plant growth and health.

Medicine

- Many biomaterials, especially heart valve replacements and blood vessels, are made of polymers like Dacron, Teflon and polyurethane.

Consumer Science

- Plastic containers of all shapes and sizes are light weight and economically less expensive than the more traditional containers. Clothing, floor coverings, garbage disposal bags, and packaging are other polymer applications.

Industry

- Automobile parts, windshields for fighter planes, pipes, tanks, packing materials, insulation, wood substitutes, adhesives, matrix for composites, and elastomers are all polymer applications used in the industrial market.

Sports

- Playground equipment, various balls, golf clubs, swimming pools, and protective helmets are often produced from polymers.

2.3 Polymerization [15-18]

The process by which polymers are formed from monomers is called polymerization. Converting monomer to long chain polymer is the final step in the polymer manufacturing sequence. It is possible to look at polymerization in at least two different ways: the nature of the catalyst used, and the way the chains grow to form the final product. Polymerizations can be conducted in the gaseous, liquid or solid state, and now in the liquid crystal state to produce highly oriented macromolecules. An appreciation of the kind of advances that have been made is important because of the new possibilities for manufacturing finished products that are becoming available.

2.4 Different Polymerization Processes

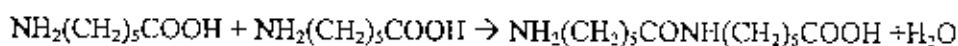
The process of polymerization may be divided into two ways (i) Chemical process and (ii) Physical process.

2.4.1 Chemical Process or Conventional polymerization process

A variety of methods are employed for producing polymer films and some of them are step growth, chain growth, addition and free radical polymerization.

Step-Growth Polymerization

In step-growth polymerization, a polymer is formed by the stepwise repetition of the same reaction over and over again. A typical example is the formation of polyamide from 6-aminocaproic acid:

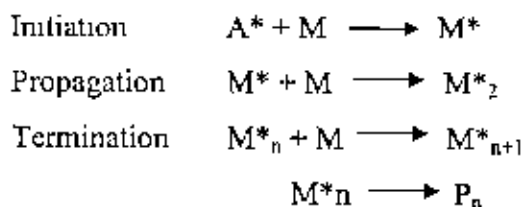


Chain-Growth Polymerization

In chain-growth polymerization a long-chain molecule is formed by a series of consecutive steps that is completed in a very short. In this case, the products are only final polymers. Unlike the case of step-growth polymerization, intermediate-size molecules cannot be isolated.

Addition Polymerization:

A typical example of chain-growth polymerization is addition polymerization, which can be schematically shown as follows:



The entire reaction is carried by the chain reaction of reactive species M^* . Depending on the nature of the reactive species, the addition polymerization is classified as free radical polymerization, ionic polymerization (cationic and anionic), and so on.

Free-Radical Polymerization

A type of polymerization, in which the propagating species is a long chain free radical, usually initiated by the attack of free radicals derived by thermal or photo-chemical decomposition of unstable materials called initiators.

Ionic Polymerization

In ionic polymerization the propagating species is a long chain of cation or anion.

Radiation Polymerization

Polymerization initiated by ionizing radiation such as γ rays from ^{60}Co or high-energy electron beams is known as radiation polymerization.

2.4.2 Physical Processes for polymer thin film deposition

The important processes of film formation are (i) Evaporation and (ii) Plasma Polymerization.

(i) Evaporation

The thermal evaporation method is simple and can produce good quantity film and hence this method becomes a good technique for thin film fabrication. Here vacuum evaporation is described, one of the physical methods, which is usually used to prepare thin film.

Vacuum Evaporation

Deposition of thin films by evaporation is very simple and convenient, and is the most widely used technique. One merely has to produce a vacuum environment in which a sufficient amount of heat is given to the evaporant to attain the vapor pressure necessary for evaporation, and then the evaporation material is allowed to condense on a substance kept at a suitable temperature.

(ii) Plasma Polymerization

As this technique is used in the preparation of the organic thin films to be investigated in the present study, a little detail about plasma and plasma polymerization is documented in the following sections.

2.5 Plasma and Plasma Polymerization [19-25]**2.5.1 Plasma**

Plasma is a partially ionized gas, in which a certain proportion of electrons are free rather than being bound to an atom or molecule. The ability of the positive and negative charges to move somewhat independently makes the plasma electrically conductive so that it responds strongly to electromagnetic fields. Plasma therefore has properties quite unlike those of solids, liquids or gases and is considered to be a distinct state of matter. Like gas,

plasma does not have a definite shape or a definite volume unless enclosed in a container, but unlike gas, in the influence of a magnetic field, it may form structures such as filaments, beams and double layers.

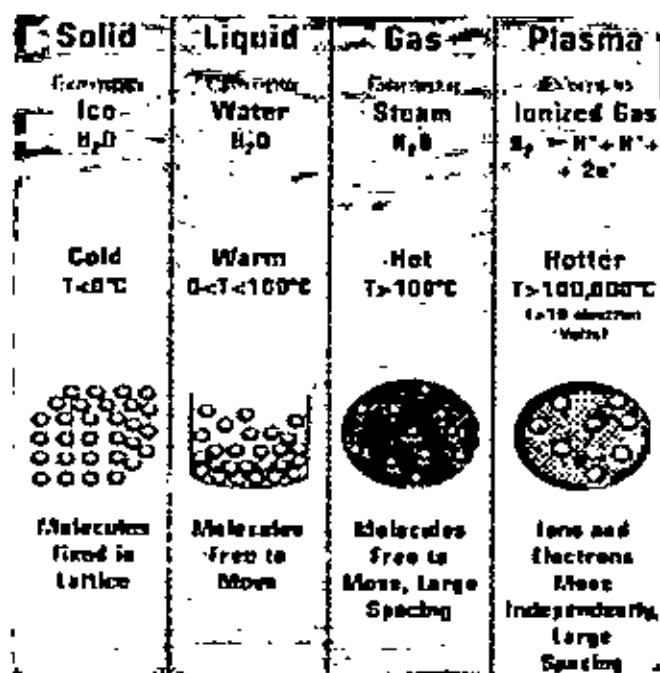


Fig 2.2 Different states of water molecules

Plasma is sometimes called "the fourth state of matter", beyond the familiar three--solid, liquid and gas. It is a gas in which atoms have been broken up into free-floating negative electrons and positive ions, atoms which have lost electrons and are left with a positive electric charge. The transition from a gas to an ionized gas, i.e., plasma, is not a phase transition, since it occurs gradually with increasing temperature. During the process, a molecular gas dissociates first into an atomic gas which, with increasing temperature, is ionized as the collisions between atoms are able to free the outermost orbital electrons. Resulting plasma consists of a mixture of neutral particles, positive ions (atoms or molecules that have lost one or more electrons), and negative electrons.

Common forms of plasma

Artificially produced plasmas are used in Plasma TVs, fluorescent lamps, corona discharge ozon generator, arc lamp, plasma torch, plasma globe, reactive ion etching etc.

Terrestrial plasmas are lightning, ball lightning, jets, ionosphere, polar aurorae, portions of fire.

Space and astrophysical plasmas are in the sun and other stars, the solar wind, the interplanetary medium, the interstellar medium, the intergalactic medium, the accretion discs.

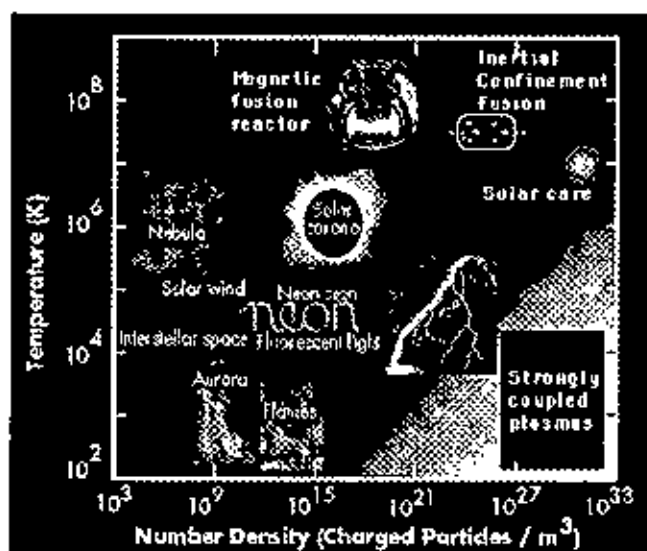


Fig 2.3 The plasma systems occur in terms of typical density and temperature conditions.

In recent years, the field of gas discharge plasma applications has rapidly expanded. The wide variety of chemical non-equilibrium conditions is possible since parameters can easily be modified such as the chemical input pressure, electromagnetic field structure, discharge configuration, and temporal behavior.

Because of this multi-dimensional parameter space of the plasma conditions, there exists a large variety of gas discharge plasmas employed in a large range of applications. Four types of plasma i.e., the glow discharge (GD), capacitively coupled (CC), inductively coupled plasma (ICP), and the micro wave-inductively plasma (MIP) are commonly used in plasma spectrochemistry and are therefore familiar to most spectrochemists. However these plasmas, as well as related gas discharges, are more widely used in technological fields.

2.5.2 FUNDAMENTALS OF GLOW DISCHARGE PROCESSES [26-33]

The glow discharge owes its name to the luminous glow of the plasma. When a sufficiently strong electric field is applied in a gaseous medium, atoms and molecules in the medium will break down electrically, permitting current to flow. The initial breakdown is created by free electrons generated by collisions. These free electrons are accelerated in the electric field. If they gain sufficient energy to cause ionization of neutral gas atoms, a chain reaction starts creating more and more free charges. The

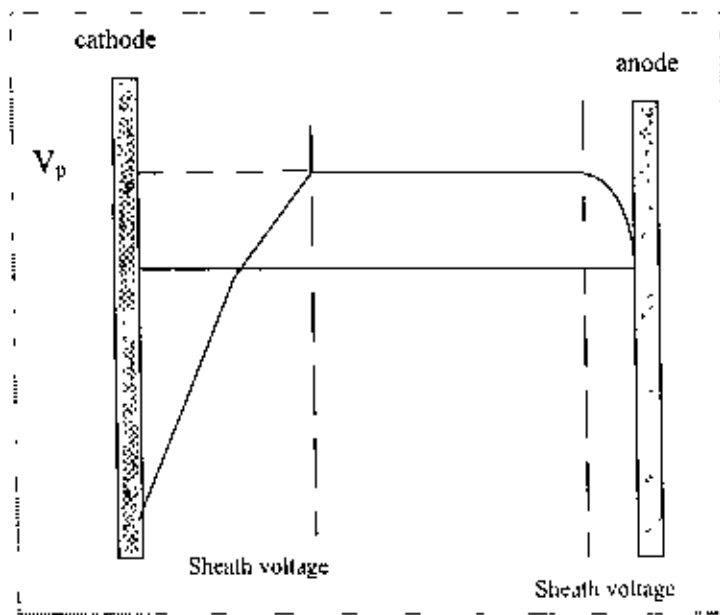


Fig 2.4 Typical setup of Glow Discharge System.

simplest glow discharge configuration consists of two parallel electrode plates being held on different electrical potential. One electrode is called **cathode** and is negatively charged, the other is the **anode**; it is on positive potential. Once the glow discharge is established the potential drops rapidly close to the cathode, varies slowly in the plasma, and changes again close to the anode. Consequently, the electric field is strong in the vicinity of the cathode and the anode. The plasma, or more precisely the negative glow is virtually field free. The electric fields in the system are restricted to sheaths adjacent to each of the electrodes. The sheath fields repel electrons, having a much higher mobility than the ions, trying to reach either electrode. In fact, the plasma potential is always higher than the adjacent walls, thus reducing the electron loss rate towards the walls.

Electrons originating at the cathode will be accelerated, collide, ionize, transfer energy, and disappear by recombination with a positively charged particle. Some electrons reach the anode and get transferred into the outside circuit.

2.5.3 Direct Current (dc) glow discharge

Plasma polymerization process takes place usually in a low temperature generated by glow discharge. The space between the electrodes becomes visible when a glow discharge is established; the actual distribution of light in the glow discharge is significant and is dependent on the current-voltage characteristics of the discharge [17, 34-36].

When a constant potential difference is applied between the cathode and anode, a continuous current will flow through the discharge; giving rise to a direct current (dc) glow discharge. In a dc glow discharge the electrodes play an essential role for sustaining the plasma by secondary electron emission. The potential difference applied between the two electrodes is generally not equally distributed between cathode and anode, but it drops almost completely in the first millimeters in front of the cathode. However, for most of the other applications of dc glow discharges (sputtering, deposition, chemical etching, analytical chemistry etc.), the distance between cathode and anode is generally short. So normally a short anode zone is present beside cathode dark space and negative glow, where the slightly positive plasma potential returns back to zero at the anode. A dc glow voltage can operate over a wide range of discharge conditions. The pressure can vary from below 1 Pa to atmospheric pressure. The product of pressure and distance (PD) between the electrodes is a better parameter to characterize the discharge. For instance, at lower pressure, the distance between cathode and anode should be longer to create a discharge with properties comparable to these of high pressure with small distance. The discharge can operate in a rare gas (most often argon or helium) or in a reactive gas (N_2 , O_2 , H_2 , CH_4 , SiH_4 , etc.), as well as in a mixture of these gases.

2.5.4 Alternating Current (ac) glow discharge

The mechanism of glow discharge generation will basically depend on frequency of the alternation. At low frequencies (60 Hz), the effect is simply to form dc glow discharges of alternating polarity. However, the frequency is higher than 6 GHz the motion of ions

can no longer follow the periodic changes in field polarity. But above 500 kHz the electrode never maintains its polarity long enough to sweep all electrons or ions, originating at the opposite electrode, out of the inter-electrode volume. In this case the regeneration of electrons and ions that are lost to the walls and the electrodes takes place within the body of the plasma. The mechanism by which electrons pick up sufficient energy to cause bond dissociation or ionization involves random collisions of electrons with gas molecules, the electron picking up an increment of energy with each collision. A free electron in a vacuum under the action of an alternating electric field oscillates with its velocity 90° out of phase with the field, which obtains no energy, on the average, from the applied field. The electron can gain energy from the field only as a consequence of elastic collisions with the gas atoms, as the electric field converts the electron's resulting random motion back to ordered oscillatory motion. Because of its interaction with the oscillating electric field, the electron gains energy on each collision until it acquires enough energy to be able to make an inelastic collision with a gas atom. In that case the process of these inelastic collisions is termed volume ionization.

Thus the transfer of energy from the electric field to electrons at high frequencies is generally accepted as that operative in microwave discharges. It has also been put forward as that applicable to the widely used rf of 13.56 MHz.

2.5.5 Plasma Polymerization

Plasma polymerization takes place in a low pressure and temperature that is produced by a glow discharge through an organic gas or vapor. Plasma polymerization depends on monomer flow rate, system pressure and discharge power among other variable parameters such as the geometry of the system, the reactivity of the starting monomer, the frequency of the excitation signal and the temperature of the substrate.

The overall power input in plasma polymerization is used for two things for creating the plasma and for fragmentation of monomer. Plasma is a direct consequence of the ionization of the gases present in the reactor and fragmentation leading to polymerization is secondary process. As increasing voltage is applied between two parallel plate electrodes, an abrupt increase in current implies the breakdown of the gases in between electrodes. High-energy electrons collide with hydrocarbon molecules to produce positive

ions, C^+ , CH^+ , CH_2^+ etc., excited molecular or atomic fragments, radicals, new components etc. Positive ions are accelerated towards cathode and produce secondary electrons in the process. Excited atoms emit photons and create glow. Since remaining positive ions also flow towards cathode, the most intense glow in the reactor is at cathode.

The positive column (space spread between cathode and anode) containing electrons, ions and radicals, is electrically neutral. This is plasma or glow discharge. The major polymer deposition occurs onto the substrate surface that makes contact with the glow. Not all glow discharges yield polymer deposition though. The plasma of Ar, Ne, O_2 , N_2 are non-polymer forming and as such can be used to maintain glow in the vacuum chamber while the monomer vapor is used efficiently for polymer conversion.

Although plasma polymerization occurs predominantly in the glow region, the volume of glow is not always the same as the volume of the reactor. Both volume of glow discharge and the intensity of glow also depend on the mode of discharge, the discharge power and the pressure of the system. Under plasma conditions, the monomer molecules undergo fragmentation and deposit as polymer molecules, and a non-polymer forming by-product like hydrogen gas is evolved. Therefore plasma polymerization of an organic monomer acts as a pump. The plasma polymer does not contain regularly repeating units, the chains are branched and are randomly terminated with a high degree of crosslinking. They

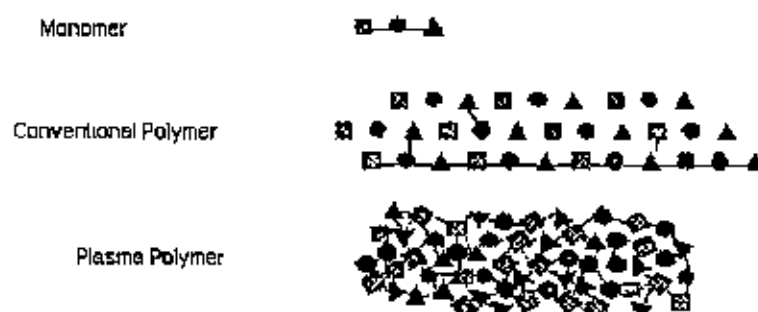


Fig 2.5 Comparison of the structures of plasma polymers and conventional polymers

adhere well to solid surfaces. Chemical reactions that occur under plasma conditions are generally very complex and nonspecific in nature. Glow discharge polymerization of organic compounds seems to proceed by the free radical mechanism and extent of ionization is small. The combination and recombination of these radicals form high molecular weight compounds called polymers. The free radicals are trapped in these films which continue to react and change the polymer network over time. Since radicals are formed by fragmentation of monomer, some elements and groups may be absent in the resulting polymer. The degree

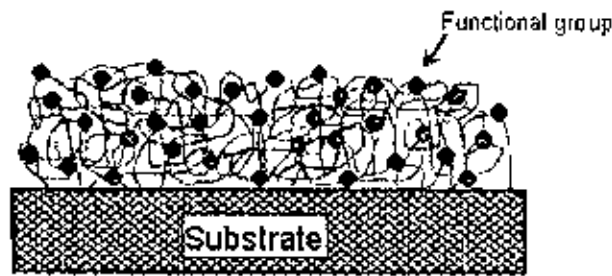


Fig 2.6 Formation of polymer with functional group

of fragmentation depends on electron density or input power and monomer flow rate. Crosslinking reactions occur on the surface or in the bulk of the newly forming plasma polymer between oligomers. The film may also be change due to reaction with oxygen and water vapor in atmosphere. The crosslinking in plasma polymer increases with the intensity and energy of bombarding ions. If the interelectrode distance is too large, then, at a given applied potential, the local electric field in the plasma will be too low to deliver sufficient energy to the electrons. The atom in a vacuum travels in straight lines. If there is residual gas in the chamber, the atoms will collide with the gas and would go in all directions losing some energy as heat. At higher pressures, the collisions will cause atoms to condense in air before reaching the substrate surface giving rise to power deposits [37].

2.6 Different types of Reactors [38]

To reach the plasma state of atoms and molecules, energy for the ionization must be input into the atoms and molecules from an external energy source. Further, the plasma state does not continue at atmospheric pressure, but at a low pressure of $1-10^{-2}$ torr. Thus, we

must provide three essential items for plasma generation: (1) an energy source for the ionization, (2) a vacuum system for maintaining a plasma state, and (3) a reaction chamber.

Generally, the electric energy for ionization of atoms and molecules is used as an energy source because of convenience of handling. Direct current (DC) commercial alternating current of a frequency of 50 or 60 Hz, and alternating current (AC) with a high frequency

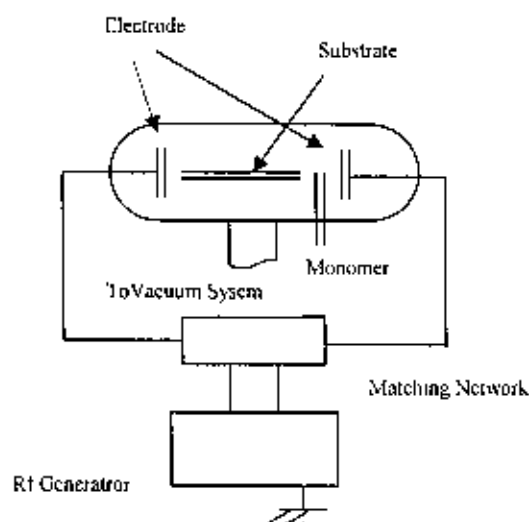


Fig 2.7 Capacitive Coupling System

of more than 60 Hz, for example, 10 or 20 kHz (audio frequency), 13.56 MHz (radio frequency) or 2.45 GHz (microwave frequency), are applicable for the electric energy. These electric powers are basically supplied to atoms and molecules in the reaction chamber from a pair of electrodes placed in the reaction chamber in a capacitive coupling manner with the electric generators. An inductive coupling manner also is possible for electric generators with a high frequency of more than 1 MHz. Basic diagrams are shown schematically in Fig 2.7, Fig 2.8 and Fig 2.9.

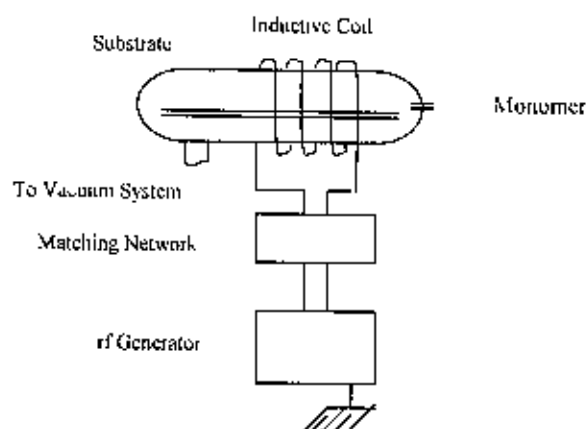


Fig 2.8 Inductive Coupling System

A vacuum system composed of a combination of a rotary pump and an oil diffusion pump is frequently used. Although using a rotary pump alone can reach low pressures of $1 \cdot 10^{-2}$ torr, using both rotary and oil diffusion pumps is desirable because of less gas remaining in the reaction chamber.

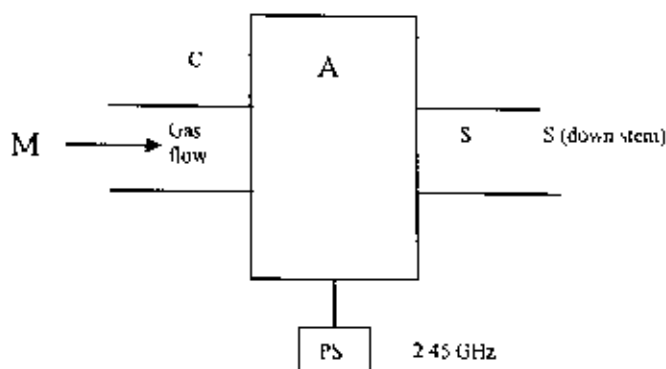


Fig 2.9 Electrode less microwave system

A design of a reaction chamber can be modified for the convenience of handling of substrates to be irradiated with plasma. A bell jar or tubular chamber made of glass or stainless steel is frequently used as a reaction chamber. A bell jar-type chamber is convenient for massive substrates, and a tubular-type chamber is better for long substrates such as fibers.

2.7 Advantages and Disadvantages of Plasma Polymers [39]

Advantages

The plasma polymerization process offers several advantages over conventional where controlling and modifying surface is important. Several advantages of plasma-polymerized films are:

The films are thin and clear. It is highly crosslinked and low solubility, excellent resistances to most chemicals, good adhesion to both metallic and plastic surfaces. Plasma polymer films can be easily produced with thickness of 500 \AA to 1 μm . Surfaces formed are relatively pinhole-free and uniformity.

Disadvantages

The main disadvantages are:

It is costly Polymerized coatings have low abrasion resistance. Low deposition rates. The process doesn't discriminate against what is coated. Everything in the coating range of the polymerization process is coated, or can become part of the coating. The process, used in mass production, is still in its infancy Contamination can be a problem and care must be exercised to prevent extraneous gases, grease films, and pump oils from entering the reaction zone. In spite of the drawbacks, plasma polymerization is far well developed process for many types of modification that simply cannot be done by any other technique.

2.8 Applications of Plasma Polymerized Organic Thin Films

Research and development of plasma and plasma-polymerized organic thin films have been undertaken very actively in the last few years and some of the products have been applied in a variety of technologies. Surface modification is probably the most important application field; plasma processes appear to have some distinct advantages compared to conventional processes. Typical uses of plasma-polymerized films are listed in Table 2.1.

Table 2.1 Potential applications of plasma-polymerized films.

Electronics devices	Integrated circuits, amorphous semiconductor, amorphous fine ceramic etching.
Electrical devices	Insulator, thin film dielectrics, separation membrane for batteries.

Polymerization: Coating of components: protective layers, hydrophobe layers, insulating layers.	All conceivable areas.
Chemical processing	Reverse osmosis membrane, perm selective membrane, gas-separation membrane-lubrication insolubilization
Artificial aging of components (tolerances of components)	Electronic industry (quartz manufacturers), environmental simulation (UV-radiation, Ozone).
Surface modification	Adhesive improvement, protective coating, abrasion-resistant coating, anti-crazing and scratching.
Bond pretreatment	Semiconductor manufacturers
Sterilization	Institutes, medicine, medicine equipment manufacturers, packing manufacturers
Cleaning / drying / reduction of excavation articles	Research institutes, museums, restorers
Optical	Anti-reflection coating, anti-dimming coating, improvement of transparency, optical fiber, optical wave guide laser and optical window, contact lens.
Textile	Anti-flammability, anti-electrostatic treatment, dying affinity, hydrophilic improvement, water repellence, shrink proofing.
Biomedical	Immobilized enzymes, organelles and cells, sustained release of drugs and pesticides, sterilization and pasteurization, artificial kidney, blood vessel.

References

- [1] <http://matse1.msc.uiuc.edu/polymers/future.html>.
- [2] <http://matse1.mse.uiuc.edu/polymers/ware.html>.

- [3] <http://www.elmhurst.edu/~chem/vchembook/400polymers.html>.
- [4] <http://www.scienceclarified.com/Ph-Py/Polymer.html>.
- [5] <http://www.chemistryexplained.com/PI-Pr/Polymers-Synthetic.html>.
- [6] <http://scifun.chem.wisc.edu/CHEMWEEK/POLYMERS/Polymers.html>.
- [7] <http://www.scienceclarified.com/Ph-Py/Polymer.html>.
- [8] <http://www.elmhurst.edu/~chem/vchembook/400polymers.html>.
- [9] Young R. J., Lovell P. A., "Introduction to polymers", Chapman & Hall, London (1991) 15.
- [10] Carraher C. E., "Polymer chemistry: an introduction", Marcel Dekker NY (1996).
- [11] Rodriguez F., Mathias L. J., Kroschwitz J., Carraher C. E., "Classroom demonstrations of polymer principles. Part I. Molecular structure and molecular mass", J. Chem. Education 65 (1988) 352 – 355.
- [12] Kaufman S. H., Falcetta, J. J., "Introduction to polymer science and technology", Johns Wiley & Sons, NY (1977) 13-23.
- [13] Allcock H. R., Lampe F. W., "Contemporary polymer chemistry", Prentice-Hall, Englewood Cliffs NJ (1981) 439-441.
- [14] <http://www.theotherpages.org/poly-faq.html#class>.
- [15] <http://openlearn.open.ac.uk/mod/resource/view.php?id=196649>.
- [16] <http://composite.about.com/library/glossary/f/bldef-f2350.htm>.
- [17] Yasuda H., "Plasma polymerization", Academic Press, Inc. NY (1985).
- [18] George J., "Preparation of thin films", Dekker Inc. NY (1992).
- [19] <http://www.phy6.org/Education/wplasma.html>.
- [20] <http://magbase.rssi.ru/REFMAN/SPPHTEXT/plasma.html>.
- [21] [http://en.wikipedia.org/wiki/Plasma_\(physics\)#Definition_of_a_plasma](http://en.wikipedia.org/wiki/Plasma_(physics)#Definition_of_a_plasma).
- [22] <http://www.plasmas.org/basics.htm>.
- [23] Lieberman M. A., Lichtenberg A. J., "Principle of plasma discharges and materials processing", John Wiley and Sons NY (1994).
- [24] Grill A., "Cold plasma in materials fabrication: from fundamentals to applications", IEEE Press NY (1994).

- [25] Bogaerts L., Wilken V., Hoffmann R., Gijbels K., Wetzig "Comparison of modeling calculations with experimental result for rf glow discharge optical emission spectroscopy", *Spectrochim. Acta Part B* 57 (2002) 109-119.
- [26] http://www.glow-discharge.com/Index.html?Discharges_1.html.
- [27] Nathan Senthil S., Muralidhar G. K., Rao Mohan G. and Mohan S., "Effect of process parameters on glow discharge and film thickness uniformity in facing target sputtering", *Thin Solid Films* 292 (1-2) (1997) 20-25.
- [28] http://en.wikipedia.org/wiki/Glow_discharge.
- [29] Hang Wei, Xiaomei Yan, Wayne David M., Olivares Jose A., Harrison W. W., Vahid Majidi, "Glow discharge source interfacing to mass analyzers: theoretical and practical considerations", *Anal. Chem.* 71 (15) (1999) 3231-3237.
- [30] <http://everything2.com/title/glow%2520discharge>.
- [31] Buntat Z., Harry J.E., Smith I.R., "Generation of a homogeneous glow discharge in air at atmospheric pressure", *Elektrika J. Elec. Engg.* 9 (2) (2007) 60-65.
- [32] <http://webh01.ua.ac.be/plasma/pages/glow-discharge.html>.
- [33] Helal A., Moustafa O.A. and Salam F.W.A., "High efficiency glow discharge ion source", *J. Nuclear and Radiation Phys.* 3 (1) (2008) 1-9.
- [34] Stark R. H., Schoenbach K. H., "Direct current high pressure glow discharge", *J. Appl. Phys.* 85 (1999) 2075-2080.
- [35] Stark R. H., Schoenbach K. H., "Direct current glow discharges in atmospheric air", *Appl. Phys. Lett.* 74 (1999) 3770-3772.
- [36] Eijkel J. C. T., Stori H. and Manz A., "A dc microplasma on a chip employed as an optical emission detector for gas chromatograph", *Anal. Chem.* 72 (2000) 2547-2552.
- [37] Gaur S. and Vergason G., "Plasma polymerization: theory and practice", *Society of Vacuum Coaters, 43rd Annual Technical Conference Proceedings*, (2000) 267-271.
- [38] Inagaki N., "Plasma surface modification and plasma polymerization", Technomic Publishing, Basel (1995).
- [39] <http://www.tungsten.com/tipspoly.pdf>.

Chapter III

Experimental Details

- 3.1 Introduction
- 3.2 The Monomer
- 3.3 Substrate and its Cleaning Process
- 3.4 Capacitively Coupled Plasma Polymerization Set-up
- 3.5 Generation of Glow Discharge Plasma in the Laboratory
- 3.6 Plasma Polymer Thin Film Deposition
- 3.7 Measurement of Thickness of Thin Films
 - 3.7.1 Multiple-beam interferometry
- 3.8 Samples for Different Measurements
- Reference

3.1 Introduction

This chapter describes the details of the monomer, substrates and their cleaning process, capacitively coupled plasma polymerization set up for thin film deposition, generation of glow discharge plasma, deposition parameters, thickness measurement and formation.

3.2 The Monomer [1]

The monomer 1-Benzyl-2-Methylimidazole (BMI) was purchased from Sigma Chemical Company (St. Louis, Mo, USA). It is a pale yellow viscous liquid. Its physical and chemical properties are given in Table 3.1.

Table 3.1 General properties of 1-Benzyl-2-Methylimidazole

Chemical formula	$C_{11}H_{12}N_2$
Physical State	Viscous liquid
Appearance	Pale yellow
Boiling point	125.0 –127.0 deg C @3mmHg
Specific Gravity / Density	1.0500g/cm ³
Molecular Weight	172.23
Solubility	Soluble in methanol and acetone
Flash point	> 110 deg C
PH, Vapor Pressure, Vapor Density, Evaporation Rate, Viscosity, Freezing / Melting Point, Decomposition Temperature, Molecular Formula	Not available

Handling: It should be avoid breathing dust, mist, or vapor, contact with eyes, skin, and clothing, should keep container tightly closed. We should avoid ingestion and inhalation and use with adequate ventilation and wash clothing before reuse.

Storage: It should be store in a cool, dry place and sin a tightly closed container.

The chemical structure of the monomer is shown in Fig 3.1.

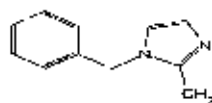


Fig 3.1 Structure of 1-Benzyl-2-Methylimidazole.

Fig 3.2 Schematic diagram of the plasma polymerization system (1 high voltage power supply, 2 pirani gage, 3 high tension leads, 4 gas inlet valve, 5 gauge head, 6 monomer injection valve, 7 flowmeter, 8 monomer container, 9 Pyrex glass dome, 10 metal electrodes, 11 electrode stands, 12 gasket, 13 lower flange, 14 bottom flange, 15 brass tube, 16 valve, 17 liquid nitrogen trap, 18 rotary pump, 19 switch and 20 variac).

i) Plasma reaction chamber

The plasma chamber consists of a cylindrical Pyrex glass bell jar having 0.15 m in inner diameter and 0.18 m in length. The top and bottom edges of the glass bell jar are covered with two rubber L-shaped (height and base 0.015 m, thickness, 0.001 m) gaskets. The cylindrical glass bell jar is placed on the lower flange. The lower flange is well fitted with the diffusion pump by a joint. The upper flange is placed on the top edge of the bell jar. The flange is made up of brass having 0.01 m in thickness and 0.25 m in diameter. On the upper flange a lay bold pressure gauge head, Edwards high vacuum gas inlet valve and a monomer injection valve are fitted. In the lower flange two highly insulated high voltages feed-through are attached housing screwed copper connectors of 0.01 m high and 0.004 m in diameter via Teflon insulation.

ii) Electrode System

In the present set-up capacitively coupled electrode system was used. Two circular stainless steel plates of diameter 0.09 m and thickness of 0.001 m are connected to the high voltage copper connectors. Moving the electrodes through the electrode stands can change the inter-electrode separation. After adjusting the distance between the electrodes they are fixed with the stands by means of screws. The substrates are usually kept on either of the electrodes for plasma deposition.

iii) Pumping Unit

For creating laboratory plasma, first step is pumping out air/gas from the plasma chamber. In this system a rotary pump of vacuubrand (Vacuubrand GMBH & Cor. Germany) is used.

iv) Vacuum Pressure Gauge

A vacuum pressure gauge head (Laybold AG) and a meter (Thermotron™ 120) of

Laybold, Germany, are used to measure inside pressure of the plasma deposition chamber.

v) Input Power for Plasma Generation

The input power supply for plasma excitation comprises of step-up high-tension transfer and a variac. The voltage ratio at the output of the high-tension transformer is about 16 times that of the output of the variac. The maximum output of the variac is 220 V and that of the transformer is about 3.5 kV with a maximum current of 100 mA. The deposition rate increases with power at first and then becomes independent of power at high power values at constant pressure and flow rate.

vi) Monomer Flowing System

The monomer flowing system consists of a conical flask of 25 ml capacity and a pyrex glass tube with capillarity at the end portion. The capillary portion is well fitted with metallic tube of the nozzle of the high vacuum needle valve. The conical flask with its components is fixed by stand-clamp arrangement.



Fig 3.3 Plasma Polymerization system in the laboratory

vii) Supporting Frame

A metal frame of dimension 1.15 m x 0.76 m x 0.09 m is fabricated with iron angle rods, which can hold the components described above. The upper and lower bases of the frame are made with polished wooden sheets. The wooden parts of the frame are varnished and the metallic parts are painted to keep it rust free. The pumping unit is placed on the lower

base of the frame. On the upper base a suitable hole is made in the wooden sheet so that the bottom flange can be fitted with nut and bolts.

3.5 Generation of Glow Discharge Plasma in the Laboratory

Glow discharges are produced by an applied static or oscillating electric field where energy is transferred to free electrons in vacuum. Inelastic collisions of the energetic free electrons with the gas molecules generate free radicals, ions, and species in electronically excited states. This process also generates more free electrons, which is necessary for a self-sustaining glow [7-10]. The excited species produced are very active and can react with the surfaces of the reactors as well as themselves in the gas phase.

The important feature of glow discharge plasma is the non-equilibrium state of the overall system. In the plasmas considered for the purpose of plasma polymerization, most of the negative charges are electrons and most of the positive charges are ions. Due to large mass difference between electrons and ions, the electrons are very mobile as compared to the nearly stationary positive ions and carry most of the current. Energetic electrons as well as ions, free radicals, and vacuum ultraviolet light can possess energies well in excess of the energy sufficient to break the bonds of typical organic monomer molecules which range from approximately 3 to 10 eV. Some typical energy of plasma species available in glow discharge as well as bond energies encountered at pressure of approximately 0.01 mbar.

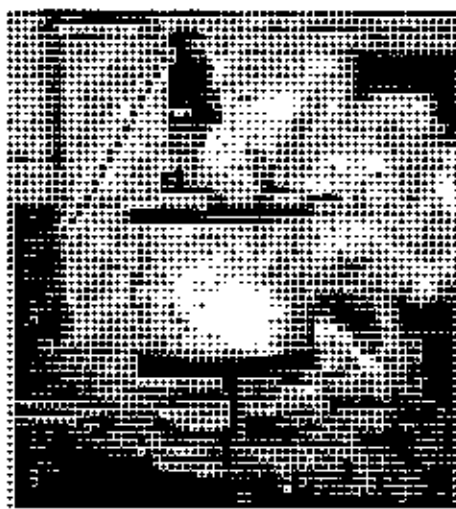


Fig 3.4 Glow discharge plasma during deposition

The important feature of glow discharge plasma is the non-equilibrium state of the overall system. In the plasma considered for the purpose of plasma polymerization, most of the negative charges are electrons and most of the positive charges are ions. Due to large mass difference between electrons and ions, the electrons are very mobile as compared to the nearly stationary positive ions and carry most of the current. Energetic electrons as well as ions, free radicals, and vacuum ultraviolet light can possess energies well in excess of the energy sufficient to break the bonds of typical organic monomer molecules which range from approximately 3 to 10 eV. Some typical energy of plasma species available in glow discharge as well as bond energies encountered at pressure of approximately 0.01 mbar.

The chamber of the plasma polymerization unit and monomer container is evacuated to about 0.01 mbar. The monomer vapor is then flown to the chamber slowly for some time. A high-tension transformer along with a variac is connected to the feed-through attached to the lower flange. While increasing the applied voltage, light bluish colors monomer plasma is produced across the electrodes at around 0.15 mbar-chamber pressure. Fig 3.3 shows the photograph of plasma deposition set-up and Fig 3.4 is the photograph of glow discharge plasma across the electrodes in the capacitively coupled parallel plate discharge chamber.

3.6 Plasma Polymer Thin Film Deposition

The electric field, when applied to the gaseous monomers at low pressures (0.01 to 1 mbar), produces active species that may react to form cross-linked polymer films. In this experiments, air was used as the primary plasma, and the monomer (1-Benzyl-2-Methylimidazole) vapor was injected downstream of the primary air glow discharge. In laboratory plasma polymerized of 1-Benzyl-2-Methylimidazole (PPBM1) thin films were prepared using a bell-jar type capacitively coupled glow discharge system described earlier. The deposition times for these were varied from 60 to 90 minutes in order to get films of different thicknesses. The optimized conditions for thin film formation for the present study:

- a) Placing the substrate on the top of the lower electrode.
- b) Maximum deposition time 1.5 hours.

- c) Electrode separation is 3.6 cm.
- d) Deposition voltage 80V.
- e) Pressure during deposition is about 1.33 Pa.

3.7 Measurement of Thickness of the Thin Films

Thickness is the single most significant film parameter. Any physical quantity related to film thickness can in principle be used to measure the film thickness. It may be measured either by several methods with varying degrees of accuracy. The methods were chosen on the basis of their convenience, simplicity and reliability. Several of the common methods are i) Multiple-Beam Interferometry ii) using a Hysteresis graph and other methods used in film-thickness determination with particular reference to their relative merits and accuracies. Multiple-Beam Interferometry technique was employed for the measurement of thickness of the thin films. This technique described below.

3.7.1 Multiple-Beam Interferometer [11]

This method utilizes the resulting interference effects when two silvered surfaces are brought close together and are subjected to optical radiation. This interference technique, which is of great value in studying surface topology in general, may be applied simply and directly to film-thickness determination. When a wedge of small angle is formed between unsilvered glass plates, which are illuminated by monochromatic light, broad fringes are seen arising from interference between the light beams reflected from the glass on the two sides of the air wedge.

Where the path difference is an integral and odd number of wavelengths, bright and dark fringes occur. If the glass surfaces of the plates are coated with highly reflecting layers, one of which is partially transparent, then the reflected fringe system consists of very fine dark lines against a bright background. A schematic diagram of the multiple beam interferometer along with a typical pattern of Fizeau fringes from a film step is shown in Fig 3.5.

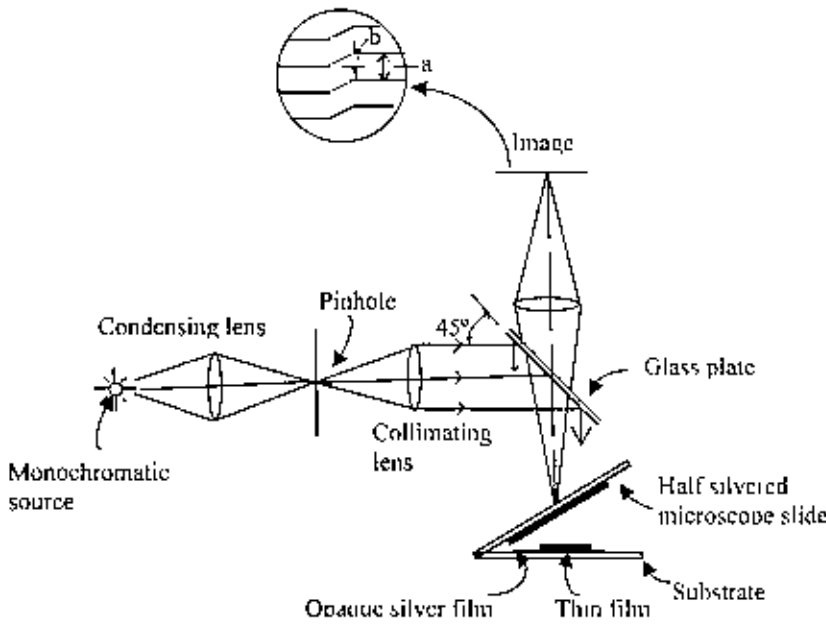


Fig 3.5 The Schematic diagram of multiple-beam interferometer.

As shown in this figure, the film whose thickness is to be measured is over coated with a silver layer to give a good reflecting surface and a half-silvered microscope slide is laid on top of the film whose thickness is to be determined. The thickness of the film d can then be determined by the relation

$$d = \frac{\lambda b}{2 a} \dots\dots\dots(3.1)$$

Where λ is the wavelength and b/a is the fractional discontinuity identified in the figure. In general, the sodium light is used, for which $\lambda=5893 \text{ \AA}$. In practice, several half-silvered slides of varying thickness and therefore of varying transmission are prepared, and one of these is selected for maximum resolution. Accurate determinations of fringe spacing are difficult and time consuming, but a method of image comparison, which considerably improves the ease and rapidity of measurement has recently been developed. Alternatively, a simple film-thickness gauge utilizing Newton's rings may be developed, which involves no critical adjustment of wedges, etc., and which reduces error in film thickness determination. In conclusion, it might be mentioned that the Tolansky method of film-thickness measurement is the most widely used and in many respects also the most accurate and satisfactory one.

3.8 Samples for Different Measurements

PPBMI thin films were deposited on to chemically cleaned glass substrates for Ultraviolet Visible spectroscopy analyses. For FTIR spectroscopy the films were scraped off from the substrate. Metal/PPBMI/Metal sandwich structures, given in chapter 6 were prepared for all sorts of electrical investigations. The experimental results are discussed in respective chapters.

References

- [1] <https://fscimage.fishersci.com/msds/99896.htm>.
- [2] Akther H. and Bhuiyan A. H., "Electrical and optical properties of plasma polymerized N, N, 3, 5 tetramethylaniline thin films", *New J. Phys.* 7 (2005) 173.
- [3] Chowdhury F.-U.-Z., Islam A B.M.O. and Bhuiyan A H , "Chemical analysis of plasma-polymerized diphenyl thin films", *Vacuum* 57 (2000) 43-50
- [4] Yasuda H., "Plasma Polymerization", Academic Press, Inc. NY (1985).
- [5] Akther H. and Bhuiyan A. H., "Space charge limited conduction in plasma polymerized N,N,3,5 tetramethylaniline thin films", *Thin Solid Films* 488 (2005) 93-97.
- [6] Anghel S.D., Frentiu T., Cordos E.A., Simon A. and Popsen A., "Atmospheric pressure capacitively coupled plasma source for the direct analysis of nonconducting solid samples", *J. Anal. At. Spectrum* 14 (1999) 541-545.
- [7] Chen F.F., "Introduction to plasma physics", Plenum Press NY (1974).
- [8] Inagaki N., "Plasma surface modification and plasma polymerization", Technomic Publishing Co. Inc. NY (1996).
- [9] Bogaerts A. and Neyts E., "Gas discharge plasma and their application", *Spectrochimica Acta Part B* 57 (2002) 609-658.
- [10] Lieberman M.A. and Lichtenberg A.J., "Principles of plasma discharges and materials processing", John Wiley and Sons, Inc. NY (1994).
- [11] Tolansky S, "Multiple beam interferometry of surface and films", Clarendon Press, Oxford (1948).

CHAPTER IV

Structural Analyses of PPBMI Thin Films

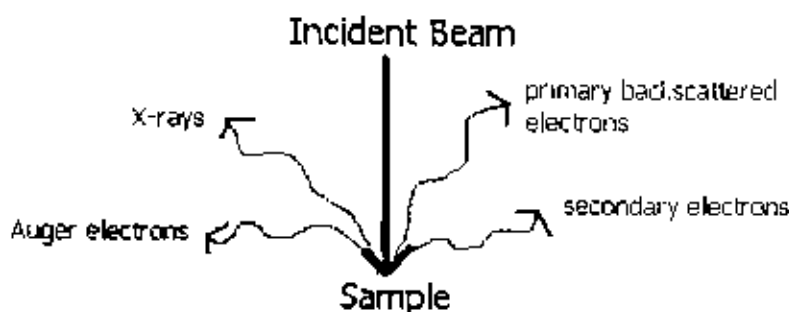
- 4.1 Introduction
- 4.2 The Scanning Electron Microscope (SEM)
 - 4.2.1 Working Principle of SEM
 - 4.2.2 Sample Preparation
 - 4.2.3 Experimental Details
 - 4.2.4 Results and Discussion
- 4.3 Fourier Transform Infrared Spectroscopy
 - 4.3.1 Typical Apparatus
 - 4.3.2 Experimental Procedure
 - 4.3.3 Results and Discussion
- References

4.1 Introduction

This chapter deals with the study of surface structure and chemical behavior of PPBMI thin films. The SEM is discussed in the beginning, and structure of PPBMI thin films studied by IR spectroscopy is discussed at the end.

4.2 Scanning Electron Microscope (SEM) [1-9]

The SEM stands for scanning electron microscope. The SEM is a microscope that uses electrons instead of light to form an image. A beam of electrons is produced at the top of the microscope by an electron gun. The electron beam follows a vertical path through the microscope, which is held within a vacuum. The beam travels through electromagnetic fields and lenses, which focus the beam down toward the sample. Once the beam hits the sample, electrons and X-rays are ejected from the sample.



Detectors collect these X-rays, backscattered electrons, and secondary electrons and convert them into a signal that is sent to a screen similar to a television screen. This produces the final image.

Since its development, SEM has developed new areas of study in the medical and physical sciences. The SEM has allowed examining a much bigger variety of specimens. The scanning electron microscope has many advantages over traditional microscopes.

The SEM has a large depth of field, which allows more of a specimen to be in focus at one time. The SEM also has much higher resolution; so closely spaced specimens can be magnified at much higher levels. Because the SEM uses electromagnets rather than lenses, the researcher has much more control in the degree of magnification. All of these

advantages, as well as the actual strikingly clear images, make the scanning electron microscope one of the most useful instruments in research today.

4.2.1 Working Procedure of SEM

A detailed explanation of how a typical SEM functions follows (refer to the diagram below):

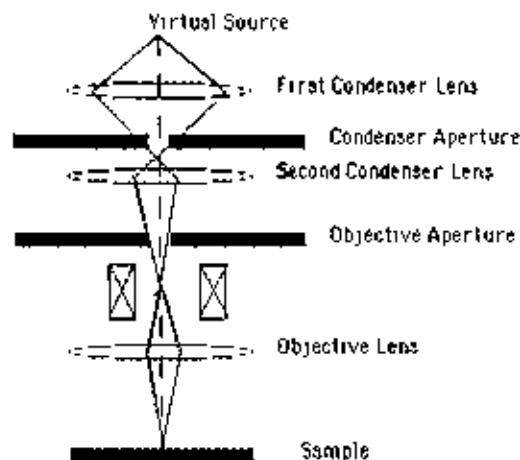


Fig 4.1 Schematic diagram of an SEM

The Virtual Source at the top represents the electron gun, producing a stream of monochromatic electrons.

1. The stream is condensed by the first condenser lens. This lens is used to both form the beam and limit the amount of current in the beam. It works in conjunction with the condenser aperture to eliminate the high-angle electrons from the beam.
2. The beam is then constricted by the condenser aperture (usually not user selectable), eliminating some high-angle electrons.
3. The second condenser lens forms the electrons into a thin, tight, coherent beam and is usually controlled by the fine probe current knob.
4. A user selectable objective aperture further eliminates high-angle electrons from the beam.
5. A set of coils then scan or sweep the beam in a grid fashion (like a television), dwelling on points for a period of time determined by the scan speed (usually in the microsecond range)
6. The final lens, the Objective, focuses the scanning beam onto the part of the specimen desired.

7. When the beam strikes the sample (and dwells for a few microseconds) interactions occur inside the sample and are detected with various instruments
8. Before the beam moves to its next dwell point these instruments count the number of interactions and display a pixel on a CRT whose intensity is determined by this number (the more reactions the brighter the pixel).
9. This process is repeated until the grid scan is finished and then repeated, the entire pattern can be scanned 30 times per second.

4.2.2 Sample Preparation

Because the SEM utilizes vacuum conditions and uses electrons to form an image, special preparations must be done to the sample. All water must be removed from the samples because the water would vaporize in the vacuum. All metals are conductive and require no preparation before being used. All non-metals need to be made conductive by covering the sample with a thin layer of conductive material. Using a device called a sputter coater does this.



Fig 4.2 SEM opened sample chamber

The sputter coater uses an electric field and argon gas. The sample is placed in a small chamber that is at a vacuum. Argon gas and an electric field cause an electron to be removed from the argon, making the atoms positively charged. The argon ions then become attracted to a negatively charged gold foil. The argon ions knock gold atoms from the surface of the gold foil. These gold atoms fall and settle onto the surface of the sample producing a thin gold coating.

4.2.3 Experimental Details

Scanning electron micrographs of the PPBMI thin films surfaces were taken using a Scanning Electron Microscope (XL-30, Philips, Netherlands). The sample surface was coated with a thin layer of gold-by-gold sputtering (AGAR Auto Sputter Coater) and placed in the microscope.

4.2.4 Results and Discussion

The scanning electron micrographs of PPBMI thin films are presented in Fig 4.3. The micrographs (a) magnification 1000x (b) magnification 5000x and (c) magnification 15000x show smooth, uniform and pinhole free surfaces of the PPBMI thin films.

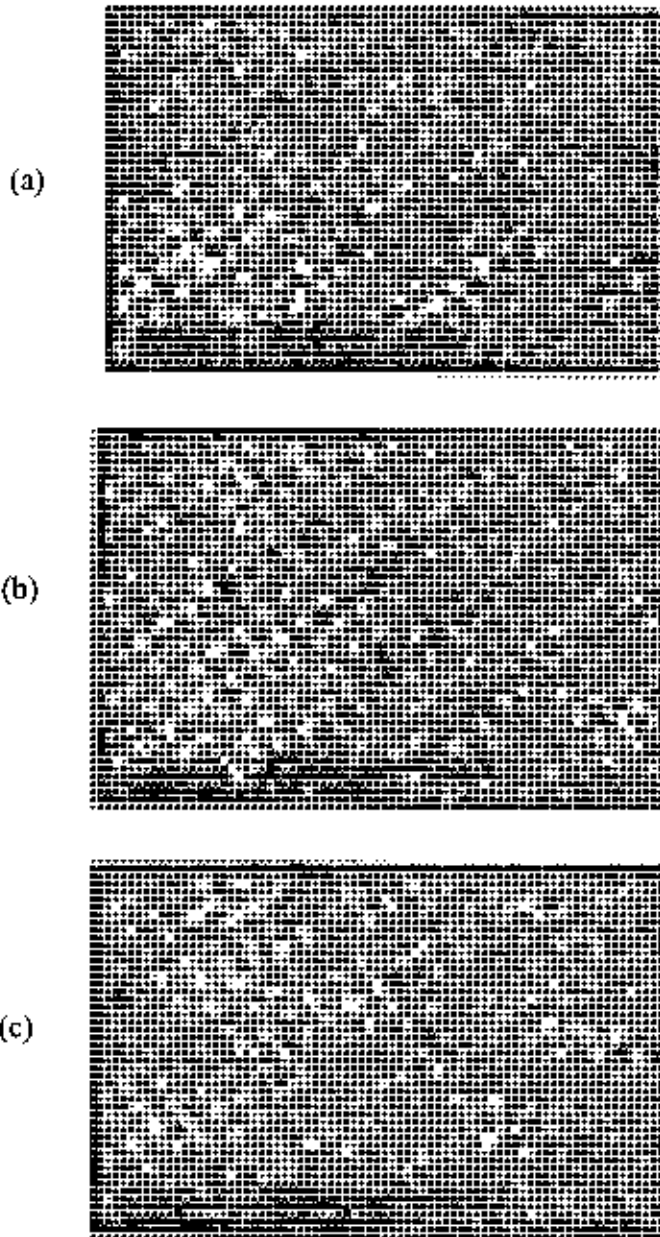


Fig 4.3 Micrographs of PPBMI thin films onto glass substrate
(a) magnification 1000x (b) magnification 5000x and (c) magnification 15000x

4.3 Fourier Transform Infrared Spectroscopy

Infrared Spectroscopy (IR Spectroscopy) is the subset of spectroscopy that deals with the infrared region of the electromagnetic spectrum. It covers a range of techniques, the most common being a form of absorption spectroscopy. It is an analytical technique for chemical compound identification. It is based on the fact that different chemical functional groups absorb infrared light at different wavelengths dependent upon the nature of the particular chemical functional group. A Fourier Transform is a mathematical conversion that allows the split of the entire infrared light spectrum simultaneously, then converting the scanning results mathematically into a wave versus absorbance spectra. Combined together these two functions provide Fourier Transform Infrared Spectroscopy (FTIR) is an instrument that can be used in the identification and characterization of organic compounds. It can be used to investigate solids as powders, films or blocks, liquids either pure or as solutions, and gases. FTIR is routinely used for forensic analysis, for example in the identification of foreign materials in food or beverage products by matching the spectra of the material in question with the spectra of known compounds.

Both inorganic and organic materials can be examined in the crude or pure state, and useful analysis can be carried out on mixtures. Materials can be examined in solid, liquid, or gaseous state. The common applications of IR includes: (i) determination of the type and amount of an impurity in an organic compound, (ii) determination of the monomer composition or microstructure of a copolymer, (iii) identification of the constituents and composition of a mixture, (iv) determination of the extent to which a reaction has proceeded, (v) determination of the structure of a compound, (vi) identification of a structure introduced in a compound by a physical treatment or environmental aging

Infrared refers to that part of the electromagnetic spectrum between the visible and microwave regions. IR is typically operated in the Mid-IR range between $4000-400\text{ cm}^{-1}$ when it is used for compound identification purposes. IR in either the Far - IR range between $400-10\text{ cm}^{-1}$ and the Near-IR $14,000-4,000\text{ cm}^{-1}$ is typically carried out for special purposes.

Infrared radiation is absorbed by organic molecules and converted into energy of molecular vibration. In IR spectroscopy, an organic molecule is exposed to infrared

radiation. When the radiant energy matches the energy of a specific molecular vibration, absorption occurs [10-13].

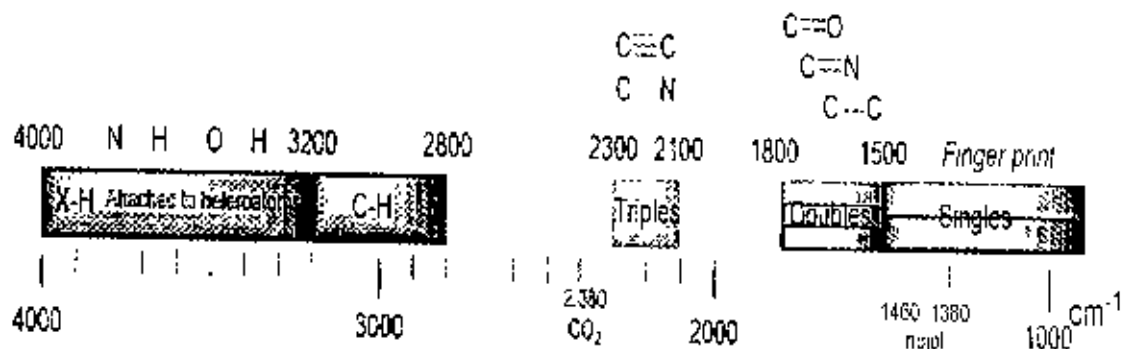


Fig 4.4 Correlation Table of Infrared Spectroscopy

IR radiation does not have enough energy to induce electronic transitions as with UV. Absorption of IR is restricted to compounds with small differences in the possible vibrational and rotational states. For a molecule to absorb IR, the vibrations or rotations within a molecule must cause a net change in the dipole moment of the molecule. The alternating electrical field of the radiation interacts with fluctuations in the dipole moment of the molecule. If the frequency of the radiation matches the vibrational frequency of the molecule then radiation will be absorbed, causing a change in the amplitude of molecular vibration.

The positions of atoms in a molecule are not fixed; they are subject to a number of different vibrations. Vibrations fall into two main categories of stretching and bending [14].

Stretching: Change in inter-atomic distance along bond axis.

Stretching vibrations

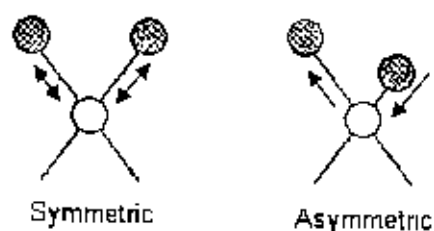


Fig 4.5 Stretching vibrations

Bending: Change in angle between two bonds. There are four types of bend:

- (i) Rocking
- (ii) Scissoring

- (iii) Wagging
- (iv) Twisting

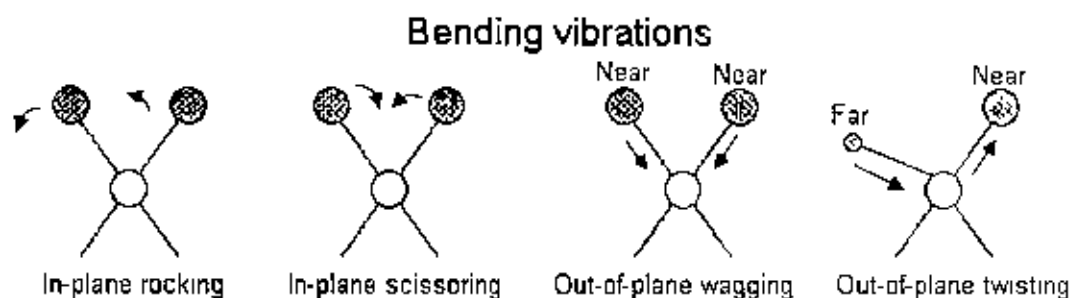


Fig 4.6 Bending vibrations

Stretching frequencies are higher than corresponding bending frequencies. (It is easier to bend a bond than to stretch or compress it.) Bonds to hydrogen have higher stretching frequencies than those to heavier atoms. Triple bonds have higher stretching frequencies than corresponding double bonds, which in turn have higher frequencies than single bonds.

The general regions of the infrared spectrum in which various kinds of vibrational bands are observed are outlined in the following chart. The upper section above the dashed line refer to stretching vibrations, and the lower section below the line encompasses bending vibrations.

4.3.1 Typical Apparatus

A beam of infrared light is produced and split into two separate beams. One is passed through the sample, the other passed through a reference which is often the substance the

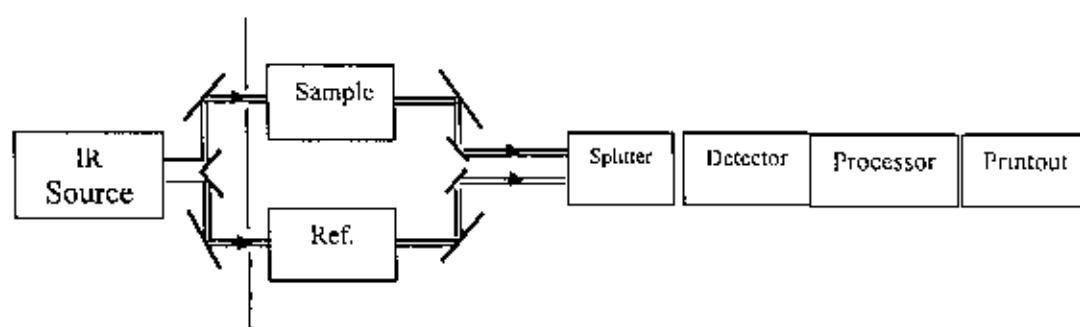


Fig 4.7 Typical IR Spectrometer setup

sample is dissolved in. The beams are both reflected back towards a detector, however first they pass through a splitter which quickly alternates which of the two beams enters the detector [15].

4.3.2 Experimental Procedure

A drop of liquid monomer was placed between two thin potassium bromide (KBr) pellets to record the FTIR spectrum. PPBMI thin film deposited on glass substrate was used for the FTIR analysis. Specimens were scraped off from the substrates and a little amount of sample was taken to prepare pellets after mixing with KBr. The strength of an FTIR absorption spectrum is dependent on the number of molecules in the beam.

FTIR spectra of the BMI and PPBMI thin films were recorded at room temperature using a double-beam IR Spectrophotometer Shimadzu –IR 470 (Shuimadzu, Tokyo, Japan). All the spectra were recorded in transmittance (%) mode in the wavenumber range is 4000-400 cm^{-1} .

4.3.3 Results and Discussion

The FTIR spectra of BMI and PPBMI thin films are represented in Fig 4.8. It shows a well matching with the standard IR spectrum of the monomer supplied by Sigma Aldrich Co., USA except for a few extra bands (3645 - 3625 cm^{-1}), which may be due to absorbed water and hydrogen bonded OH stretching. The characteristic absorption band at 3030 cm^{-1} may be assigned to aromatic C-H stretching vibration. The bands observed at 2928 and 2872 cm^{-1} in the monomer spectrum may be attributed to CH_2 and CH_3 asymmetric and symmetric stretching vibrations respectively. There are some overtones or a combination of bands in the 2000-1800 cm^{-1} region. The strong absorption bands between 1634 -1496 and 1454-1427 cm^{-1} are due to C=C and C=N stretching vibrations in the aromatic ring respectively. The absorption bands between 1358 and 986 cm^{-1} indicate C-H in plane (symmetrical) bending vibration in BMI. The sharp absorption peaks at 727 and 698 cm^{-1} are due to C-H out-of-plane bending vibrations. The absorptions at 631 cm^{-1} indicate C=C out of plane bending. The FTIR spectrum of the

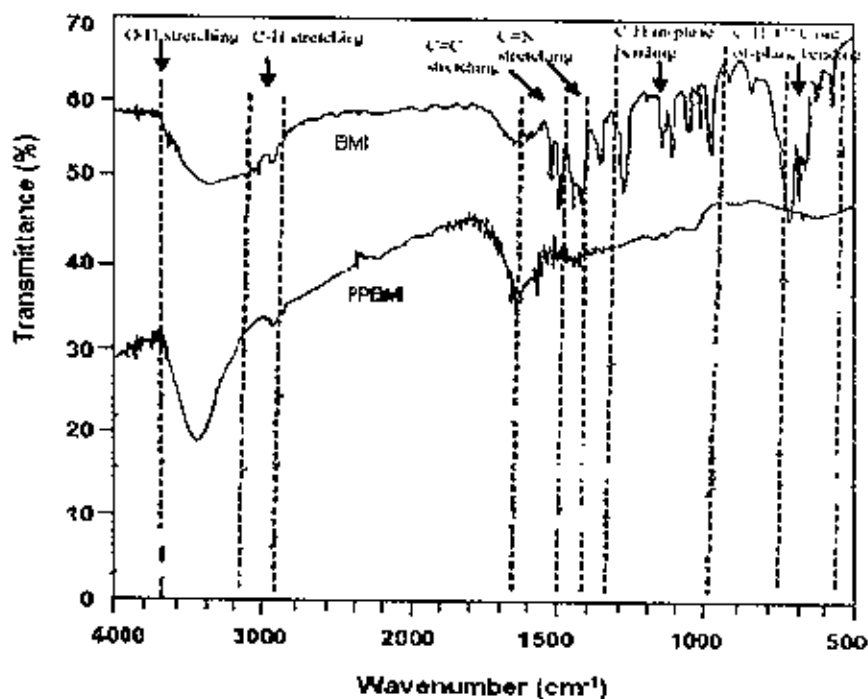


Fig 4.8 The FTIR spectra of BMI and PPBMI thin films (Curves are linearly shifted upward for convenience)

PPBMI thin films are not well resolved compared to that of BMI. It is observed that a new prominent band at 3421 cm^{-1} corresponding to O-H stretching has arisen due to absorbed water. It is plausible because the PPBMI thin films react with oxygen when exposed to atmosphere. The characteristic absorption bands at 3030 cm^{-1} presented in the monomer spectrum due to C-H stretching vibration is not present in this spectrum. The absence of C-H band (3030 cm^{-1} and $727 - 677\text{ cm}^{-1}$) may be due to the chain formation in abstraction of H from monomer structure. The absorption bands assigned to CH_2 and CH_3 stretching vibrations are shifted to 2924 and 2854 cm^{-1} compared to that of the monomer. The absorption bands between 1653 and 1610 cm^{-1} present in spectra is due to C=C aromatic stretching vibrations. The absorption band due to C=C stretching vibrations within $1636\text{-}1611\text{ cm}^{-1}$ is shifted slightly to higher frequency with higher intensity in PPBMI spectrum. This may be due to inclusion of oxygen as C=O in the structure along with some conjugation. The strong absorption band for C-H in-plane bending at 1283 cm^{-1} in the monomer spectrum is shifted to 1273 cm^{-1} and become very weak in the PPBMI. The absorption band present at 1024 cm^{-1} due to C-H in-plane bending becomes very weak compared to 1030 cm^{-1} in the monomer.

Table 4.1 Assignments of FTIR absorption bands for BMI and PPBMI thin film.

Band	Wavenumber (cm ⁻¹)	
	BMI	PPBMI
O-H stretching	3645 - 3626	3421
C-H aromatic stretching	3030	-
CH ₂ asymmetric stretching	2928	2924
CH ₃ symmetric stretching	2872	2854
C=O stretching vibration	-	1700
C=C stretching vibration	1634 -1496	1653 -1610
C=N stretching vibration	1454-1427	1436, 1419
C-H in-plane bending vibrations	1358-986	1273
C-H out-of-plane bending vibrations	727 - 677	-
C=C out-of-plane bending	631 - 575	577

From the FTIR analysis, it is revealed that the chemical structure of PPBMI thin films consists of aromatic conjugated chains which are formed due to abstraction of hydrogen. It is also evident that hydroxyl and carbonyl groups is present owing to the exposure of PPBMI thin films to the atmosphere after deposition and during experimentation. So, the structure of PPBMI thin films is chemically some what different from that of BMI monomer.

References

- [1] Suzuki E., "High-resolution scanning electron microscopy of immunogold-labelled cells by the use of thin plasma coating of osmium", *J. Microscopy* 208 (3) (2002) 153–157.
- [2] Malick Linda E., Wilson Richard B., Stetson David, "Modified Thiocarbonylhydrazide procedure for scanning electron microscopy: routine use for normal, pathological, or experimental tissues". *Biotechnic and Histochemistry* 50 (4) (1975) 265–269.
- [3] Jeffrey C. E., Read N. D., "Ambient- and Low-temperature scanning electron microscopy", London Academic Press (1991) 313–413.

- [4] Russell S. D., Daghan C. P., "Scanning electron microscopic observations on deembedded biological tissue sections: Comparison of different fixatives and embedding materials". *J. Elec. Microscopy Technique* 2 (5) (1985) 489–495.
- [5] Wergin W. P., Erbe E. F., "Snow crystals: capturing snow flakes for observation with the low-temperature scanning electron microscope". *Scanning* 16 (Suppl. IV): IV88–IV89 (1994).
- [6] Barnes P. R. F., Mulvaney R., Wolff E. W., Robinson K. A., "A technique for the examination of polar ice using the scanning electron microscope". *J. Microscopy* 205 (2) (2002) 118–124.
- [7] Goldstein G. I., Newbury D. E., Echlin P., Joy D. C., Fiori C., Lifshin E. "Scanning electron microscopy and x-ray microanalysis", Plenum Press NY (1981).
- [8] Danilatos G. D., "Foundations of environmental scanning electron microscopy". *Advances in Electronics and Electron Phys.* 71 (1988) 109–250.
- [9] http://en.wikipedia.org/wiki/File:SEM_chamber1.JPG.
- [10] http://en.wikipedia.org/wiki/infrared_spectroscopy.
- [11] Smith B.C., "Fundamentals of fourier transform infrared spectroscopy", CRC, Boca Raton, FL, USA (1996).
- [12] Coleman P., "Practical sampling techniques for infrared spectroscopy", CRC, Boca Raton, FL, USA (1993).
- [13] <http://orgchem.colorado.edu/hndbksupport/irtutor/tutorial.html>.
- [14] <http://teaching.shu.ac.uk/hwb/chemistry/tutorials/molspec/irspec1.htm>.
- [15] http://en.wikipedia.org/wiki/File:IR_spectroscopy_apparatus.jpeg.

CHAPTER V

Ultraviolet-Visible Spectroscopy of PPBMI Thin Films

- 5.1 Introduction
 - 5.2 Ultraviolet-Visible (UV-Vis) Spectroscopy
 - 5.2.1 The Electromagnetic Spectrum
 - 5.2.2 Electronic Transitions
 - 5.3 The Absorption Law
 - 5.3.1 Beer-Lambert Law
 - 5.4 Instrumentation - Ultraviolet-visible spectrophotometer
 - 5.5 Results and Discussion
- References

5.1 Introduction

The ultraviolet-visible (UV-Vis) spectroscopic analysis of PPBMI thin films is presented in this chapter. The absorbance, absorption coefficient, direct and indirect transition energy gaps, extinction coefficient for PPBMI thin films are discussed.

5.2 Ultraviolet-visible (UV-Vis) Spectroscopy

UV-Vis involves the spectroscopy of photons in UV-region. This means it uses light in the visible and adjacent (near ultraviolet and near infrared) ranges. The absorption in the visible ranges directly affects the color of the chemicals involved. In this region of the electromagnetic spectrum, molecules undergo electronic transitions. This technique is complementary to fluorescence spectroscopy, in that fluorescence deals with transitions from the excited state to the ground state, while absorption measures transitions from the ground state to the excited state [1].

UV-Vis spectroscopy is useful as an analytical technique for two reasons. First it can be used to identify some functional groups in molecules and secondly, it can be used for assaying. This second role determining the content and strength of a substance is extremely useful [2].

It corresponds to electronic excitations between the energy levels that correspond to the molecular orbitals of the systems. In particular, transitions involving π orbitals and lone pairs (n = non-bonding) are important and so UV-Vis spectroscopy is of the most use for identifying conjugated systems that tend to have stronger absorptions. The lowest energy transition is that between the highest occupied molecular orbital (HOMO) and the lowest unoccupied molecular orbital (LUMO) in the ground state. The absorption of the EM radiation excites an electron to the LUMO and creates an excited state. The more highly conjugated the system, the smaller the HOMO-LUMO gap, ΔE , and therefore the lower the frequency and longer the wavelength, λ . The unit of the molecule that is responsible for the absorption is called the chromophore [3].

5.2.1 The Electromagnetic Spectrum

The visible spectrum constitutes but a small part of the total radiation spectrum. Most of the radiation that surrounds us cannot be seen, but can be detected by dedicated sensing instruments. This electromagnetic spectrum ranges from very short wavelengths

(including gamma and x-rays) to very long wavelengths (including microwaves and broadcast radio waves).

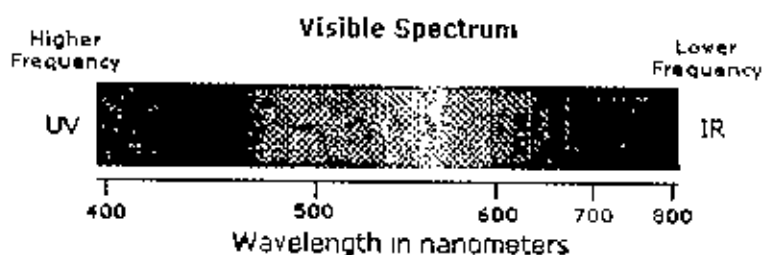


Fig 5.1 Visible part of the Electromagnetic Spectrum

5.2.2 Electronic Transitions

The absorption of UV or visible radiation corresponds to the excitation of outer electrons.

There are three types of electronic transition, which can be considered:

- (i) Transitions involving π , σ , and n electrons
- (ii) Transitions involving charge-transfer electrons
- (iii) Transitions involving d and f electrons

When an atom or molecule absorbs energy, electrons are promoted from their ground state to an excited state. In a molecule, the atoms can rotate and vibrate with respect to each other. These vibrations and rotations also have discrete energy levels, which can be considered as being packed on top of each electronic level.

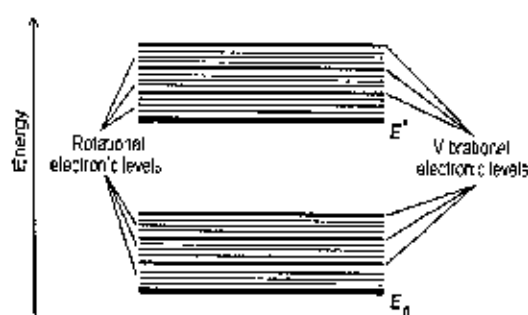


Fig 5.2 Vibration and rotational energy levels of absorbing materials

Absorbing species containing π , σ , and n electrons

Absorption of ultraviolet and visible radiation in organic molecules is restricted to certain functional groups (chromophores) that contain valence electrons of low excitation

energy. The spectrum of a molecule containing these chromophores is complex. This is because the superposition of rotational and vibrational transitions gives a combination of overlapping lines. This appears as a continuous absorption band.

Possible electronic transitions of π , σ , and n electrons are:

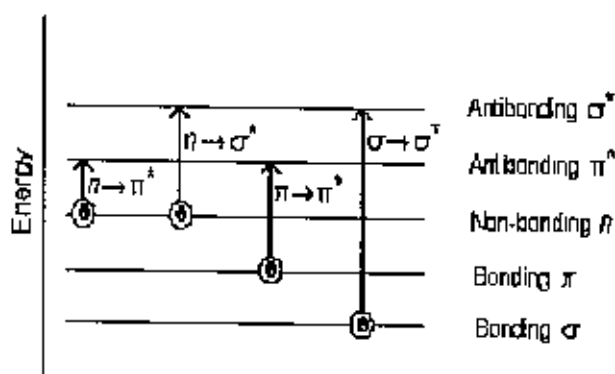


Fig 5.3 Summary of electronic energy levels.

$\sigma \rightarrow \sigma^*$ Transitions

An electron in a bonding σ orbital is excited to the corresponding antibonding orbital. The energy required is large. Absorption maxima due to $\sigma \rightarrow \sigma^*$ transitions are not seen in typical UV-Vis spectra (200–800 nm).

$n \rightarrow \sigma^*$ Transitions

Saturated compounds containing atoms with lone pairs (non-bonding electrons) are capable of $n \rightarrow \sigma^*$ transitions. These transitions usually need less energy than $\sigma \rightarrow \sigma^*$ transitions. They can be initiated by light whose wavelength is in the range 150–250 nm. The number of organic functional groups with $n \rightarrow \sigma^*$ peaks in the UV region is small.

$n \rightarrow \pi^*$ and $\pi \rightarrow \pi^*$ Transitions

Most absorption spectroscopy of organic compounds is based on transitions of n or π electrons to the π^* excited state. This is because the absorption peaks for these transitions fall in an experimentally convenient region of the spectrum (200–800 nm). These transitions need an unsaturated group in the molecule to provide the π electrons.

Molar absorptivities from $n \rightarrow \pi^*$ transitions are relatively low, and range from 10 to 100 $\text{L mol}^{-1}\text{cm}^{-1}$. $\pi \rightarrow \pi^*$ transitions normally give molar absorptivities between 1000 and

$10,000 \text{ L mol}^{-1}\text{cm}^{-1}$. The energy required for various transitions obey the following order:



The solvent in which the absorbing species is dissolved also has an effect on the spectrum of the species. Peaks resulting from $n \rightarrow \pi^*$ transitions are shifted to shorter wavelengths (blue shift) with increasing solvent polarity. This arises from increased solvation of the lone pair, which lowers the energy of the n orbital. Often (but not always), the reverse (i.e. red shift) is seen for $\pi \rightarrow \pi^*$ transitions. This is caused by attractive polarization forces between the solvent and the absorber, which lower the energy levels of both the excited and unexcited states. This effect is greater for excited state, and so the energy difference between the excited and unexcited states is slightly reduced—resulting in a small red shift. This effect also influences $n \rightarrow \pi^*$ transitions but is overshadowed by the blue shift resulting from solvation of lone pairs [4].

5.3 The Absorption Law

Many compounds absorb ultraviolet (UV) or visible (Vis.) light. The diagram below shows a beam of monochromatic radiation of radiant power P_0 , directed at a sample.. Absorption takes place and the beam of radiation leaving the sample has radiant power P .



The amount of radiation absorbed may be measured in a number of ways:

$$\text{Transmittance, } T = P/P_0$$

$$\% \text{ Transmittance, } \%T = 100 T$$

$$\text{Absorbance, } A = \log_{10} P_0/P$$

$$A = \log_{10} 1/T$$

$$A = \log_{10} 100/\%T$$

$$A = 2 - \log_{10} \%T$$

The equation, $A=2\cdot\log_{10}\%T$ allows to easily calculate absorbance from percentage transmittance data.

So, if all the light passes through a solution without any absorption, then absorbance is zero, and percentage transmittance is 100%. If all the light is absorbed, then percent transmittance is zero, and absorption is infinite [5].

5.3.1 The Beer-Lambert Law

Two empirical laws have been formulated about the absorption intensity. Lambert's law states that the fraction of the incident light absorbed is independent of the intensity of the intensity of the source. Beer's law states that the absorption is proportional to the number of absorbing molecules [6]. For most spectra the solution obeys Beer's Law. This is only true for dilute solutions. Combining these two laws gives the Beer-Lambert law:

$$I=I_0e^{-\alpha d} \dots\dots\dots(5.1)$$

$$\log_e\left(\frac{I_0}{I}\right) = \alpha d \dots\dots\dots(5.2)$$

Where I_0 is the intensity of the incident radiation, I is the intensity of the transmitted radiation, d is the path length of the absorbing species and α is the absorption coefficient. The absorption spectrum can be analyzed by Beer-Lambert law, which governs the absorption of light by the molecules. It states that, "When a beam of monochromatic radiation passes through a homogeneous absorbing medium the rate of decrease in intensity of electromagnetic radiation in UV-VIS region with thickness of the absorbing medium is proportional to the intensity coincident radiation".

The absorption co-efficient α , can be calculated from the absorption data using the relation (5.2) [7,8].

$$\alpha = \frac{2.303A}{d} \dots\dots\dots(5.3)$$

where $A = \log_{10}\left(\frac{I_0}{I}\right)$ is the Absorbance.

The relation of extinction co-efficient k with α is

$$\alpha = 4\pi k/\lambda \dots\dots\dots(5.4)$$

where λ is the wavelength.

To estimate the nature of absorption a random phase model is used where the momentum selection rule is completely relaxed. The integrated density of states $N(E)$ has been used and defined by

$$N(E) = \int_{-\infty}^{\infty} g(E) dE \dots \dots \dots (5.5)$$

The density of states per unit energy interval may be represented by $g(E) = \frac{1}{V} \sum \delta(E - E_n)$, where V is the volume, E is energy at which $g(E)$ is to be evaluated and E_n is the energy of the n th state.

If $g_v \propto E^p$ and $g_c(E) \propto (E - E_{opt})^q$, where energies are measured from the valance band mobility edge in the conduction band (mobility gap), and substituting these values into an expression for the random phase approximation, the relationship obtained $\nu^2 I_2(\nu) \propto (h\nu - E_0)^{p+q+1}$, where $I_2(\nu)$ is the imaginary part of the complex permittivity. If the density of states of both band edges is parabolic, then the photon energy dependence of the absorption becomes $\alpha\nu \propto \nu^2 I_2(\nu) \propto (h\nu - E_{opt})^2$. So for higher photon energies the simplified general equation is

$$\alpha h\nu = B(h\nu - E_{opt})^n$$

Where $h\nu$ is the energy of absorbed light, n is the parameter connected with distribution of the density of states and B is the proportionality factor. The index n equals $\frac{1}{2}$ and 2 for allowed direct transition and indirect transition energy gaps respectively [9].

Thus, from the straight-line plots of $(\alpha h\nu)^2$ versus $h\nu$ and $(\alpha h\nu)^{1/2}$ versus $h\nu$ the direct and indirect energy gaps of insulators and / or dielectrics can be determined.

5.4 Instrumentation – Ultraviolet visible spectrophotometer

The instrument used in ultraviolet-visible spectroscopy is called a UV-VIS spectrophotometer. It measures the intensity of light passing through a sample (I), and compares it to the intensity of light before it passes through the sample (I_0). A diagram of the components of a typical spectrometer is shown in the following diagram. The functioning of this instrument is relatively straightforward. A beam of light from a visible or UV light source is separated into its component wavelengths by a prism or diffraction grating. Each monochromatic beam in turn is split into two equal intensity beams by a

half-mirrored device. One beam, the sample beam, passes through a small transparent container containing a solution of the compound being studied in a transparent solvent. The other beam, reference, passes through an identical cuvette containing only the solvent. Electronic detectors then measure the intensities of these light beams

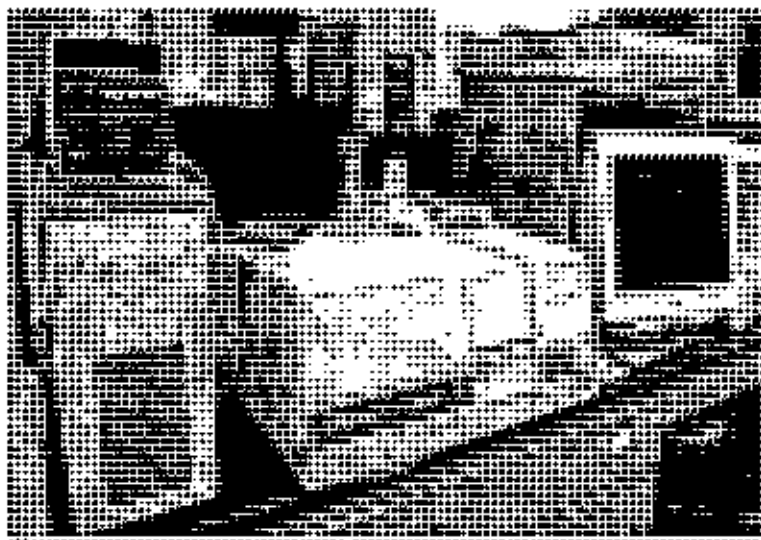


Fig 5.4 Beckman DU640 UV-Vis spectrophotometer

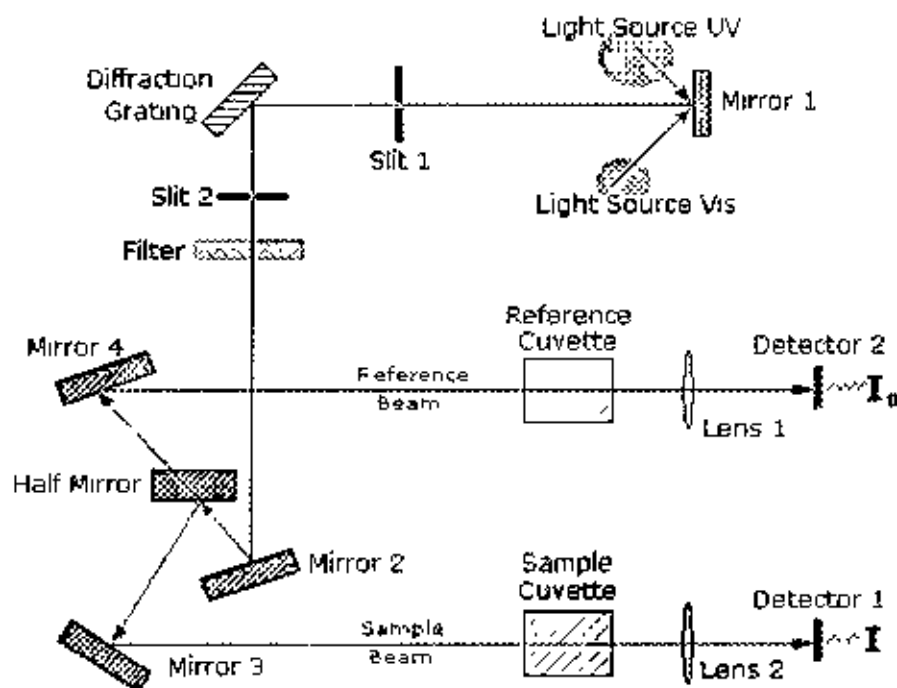


Fig 5.5 Diagram of the components of a typical spectrometer

and compared. The intensity of the reference beam, which should have suffered little or no light absorption, is defined as I_0 . The intensity of the sample beam is defined as I . Over a short period of time, the spectrometer automatically scans all the component wavelengths. The ultraviolet (UV) region scanned is normally from 200 nm to 400 nm, and the visible portion is from 400 to 800 nm [10].

5.5 Results and Discussion

Fig 5.6 shows the variation of absorbance with wavelength of BMI liquid and PPBMI thin films. It is seen that the absorbance increases with increasing thickness of the thin films and the absorption peak broadens as thickness increases. There is sharp rising of absorption in the wavelength range from 280 to 320 nm, rapid decrease of absorption in the range from 320 to 500 nm and then that decreases above 500 nm.

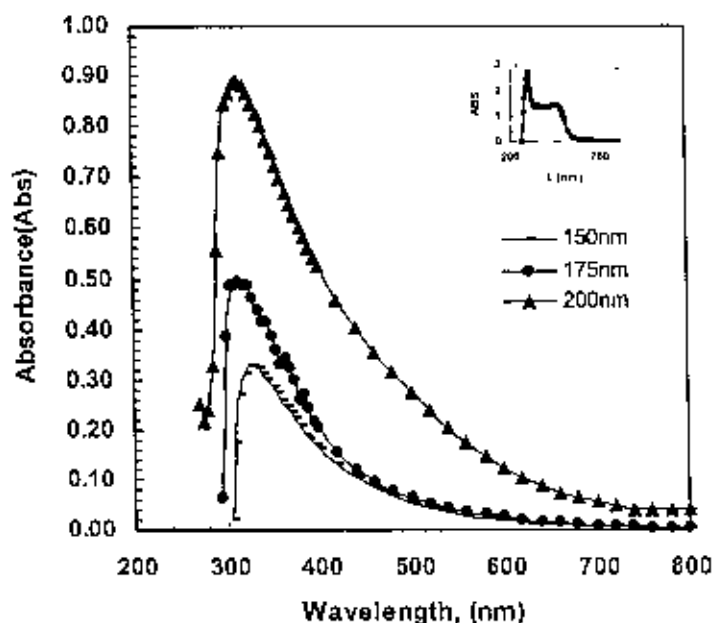


Fig 5.6 Variation of absorbance, ABS, with wavelength, λ , inset (monomer) of PPBMI thin films of different thicknesses.

It is observed that the absorption peaks of PPBMI thin films shift to higher wavelength compared to the peak of BMI (295 nm, inset of Fig 5.6). Thus there is a red shift of the absorption peak of PPBMI thin films in comparison to BMI. It is well known that presence of conjugation generally moves the absorption maximum to longer wavelength

[11]. This red shift in PPBMI thin films may demonstrate presence of conjugation in the resulting films.

The dependence of absorption coefficient on photon energy is presented in Fig 5.7. It is revealed that in low energy region the edges follow an exponential fall for values of α below about 10000 cm^{-1} . So the curves have two different slopes indicating the presence of direct and indirect transitions in PPBMI thin films. These exponential falling edges may either be due to lack of long-range order or due to the presence of defects in the thin films [11].

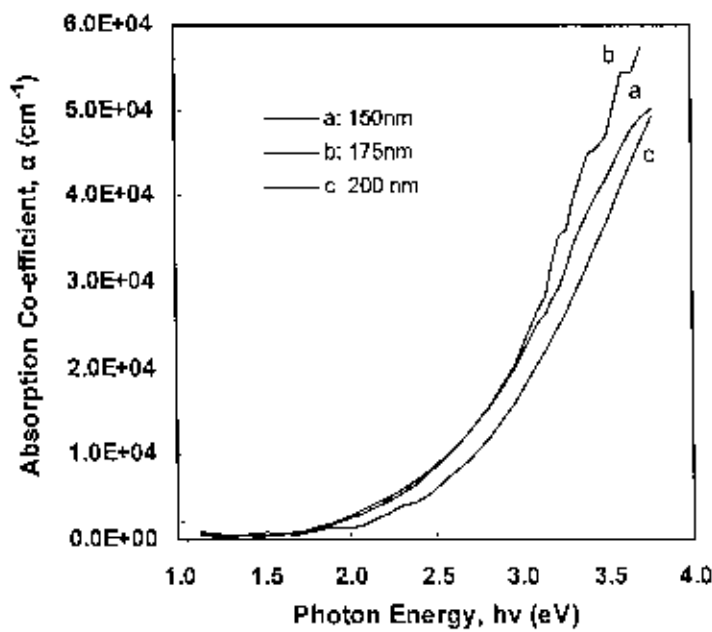


Fig 5.7 Absorption co-efficient, α , as a function of photon energy, $h\nu$, for PPBMI thin films of different thicknesses.

$(\alpha h\nu)^2$ as a function of photon energy, $h\nu$, is plotted in Fig 5.8 by which the allowed direct transition energy gap (E_{qd}) is calculated. E_{qd} is determined from the intercept of the extrapolation of the curve to zero α in the photon energy axis. In Fig 5.9 $(\alpha h\nu)^{1/2}$ as a function of photon energy, $h\nu$, is plotted to obtain the allowed indirect transition energy gap (E_{qi}). The values of E_{qd} and E_{qi} obtained from the plots of Figs 5.8 and 5.9 are given in Table 5.1. In the table, it is seen that the band gap values are not very much dependent on the film thickness used in the present investigation.

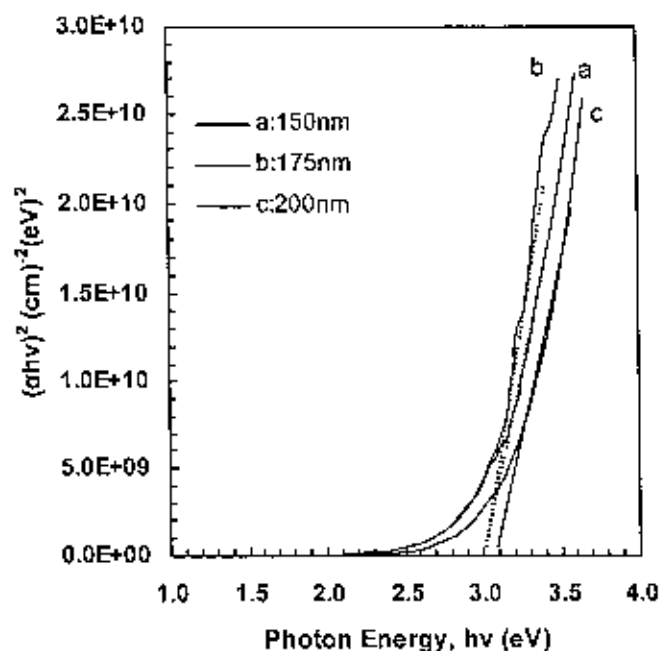


Fig 5.8 $(\alpha h\nu)^2$ versus $h\nu$ curve for PPBMI thin films.

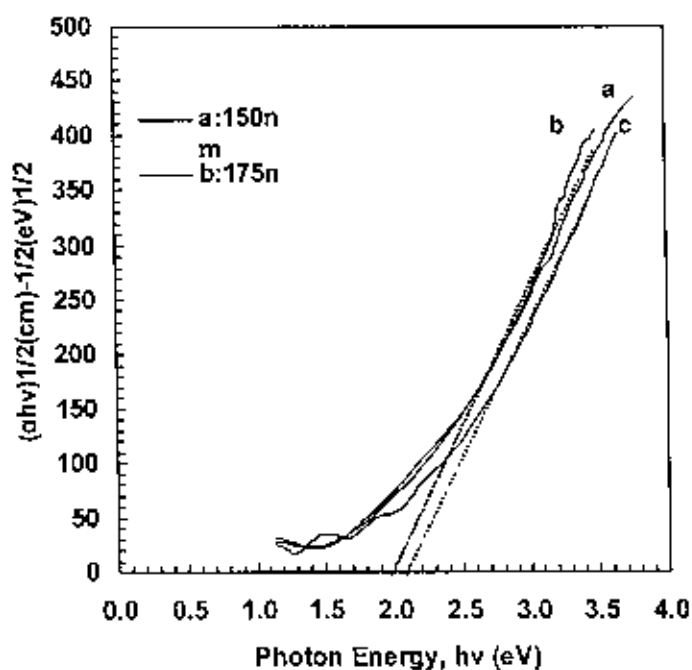
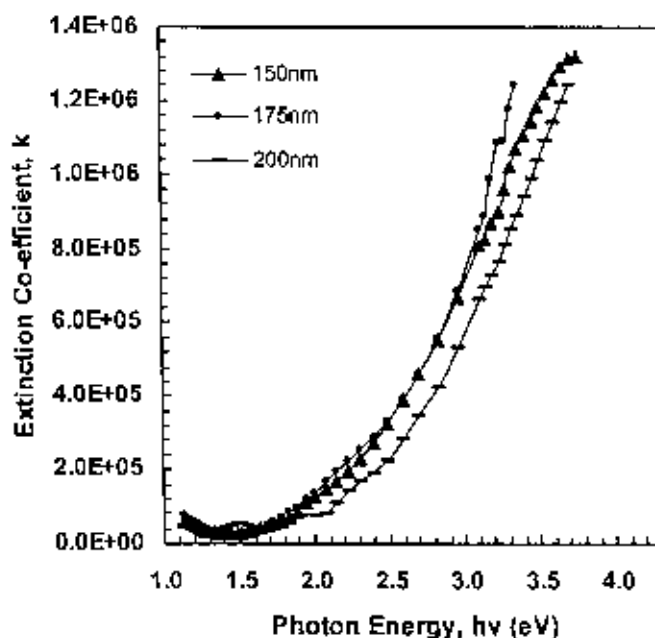


Fig 5.9 $(\alpha h\nu)^{1/2}$ versus $h\nu$ curve for PPBMI thin films.

Table 5.1 Values of allowed direct and indirect transition energy gaps

Sample	Film Thickness d (nm)	Temperature T (K)	Direct Transition energy gap, E_{qd} (eV)	Indirect Transition energy gap, E_{qi} (eV)
PPBMI	150	300	3.00	2.00
	175		3.00	2.00
	200		3.10	2.10

Physical processes that control behavior of gap states in non-crystalline materials are structural disorder responsible in the tail states and structural defects in deep states [11]. The Tauc parameter, B is a measure of the steepness of band tail (Urbach region) density of states. Comparatively a higher value of B in this film may be due to less structural disorder. The value of B calculated for PPBMI thin films is about $260 \text{ (cm)}^{-1/2}(\text{eV})^{-1/2}$. The variation of the extinction co-efficient, k with photon energy, $h\nu$, is shown in Fig 5.10. It is seen that the value of k increases with increasing photon energy which indicates that the probability of electron transfer across the mobility gap rises with the photon energy.

Fig 5.10 Plot of extinction co-efficient, k , as a function of $h\nu$ for PPBMI thin films.

107368

References

- [1] http://en.wikipedia.org/wiki/cite_note-0#cite_note-0
- [2] http://www.rsc.org/education/teachers/learnnet/pdf/LearnNet/rsc/UV_txt.pdf
- [3] <http://www.chem.ucalgary.ca/courses/350/Carey/Ch13/basics#basics>.
- [4] <http://teaching.shu.ac.uk/hwb/chemistry/tutorials/molspec/uvvisab1.htm>.
- [5] <http://teaching.shu.ac.uk/hwb/chemistry/tutorials/molspec/beers1.htm>.
- [6] Yasuda H., Marsh H. C., Bumgarner M. O. and Morosoff N., "Polymerization of organic compounds in an electrodeless glow discharge. VI. Acetylene with unusual comonomers", *J. Appl. Polym. Sci.* 19 (1975) 2845.
- [7] Chakrabarti K., Basu M., Chaudhuri S., Pal A.K., Hanzawa H. "Mechanical, electrical and optical properties of a-C:H:N films deposited by plasma CVD technique", *Vacuum* 53 3 (1999) 405-413
- [8] Nakagawa K., "Optical anisotropy of polyimide", *J. Appl. Polym. Sci.* 41 9 (1990) 2049-2058
- [9] Davis E. A. and Mott N. F., "Conduction in non-crystalline systems V. Conductivity, optical absorption and photoconductivity in amorphous semiconductors", *Phil. Mag.* 22 (1970) 903-922.
- [10] <http://www.cem.msu.edu/~reusch/VirtualText/Spectrpy/UV-Vis/uv1>.
- [11] Hu X., Zhao X.Y., Uddin A., Lee C.B., "Preparation, characterization and electronic and optical properties of plasma-polymerized nitriles", *Thin Solid Films* 477 (2005) 81-87.

CHAPTER VI

AC Electrical Properties of PPBMI Thin Films

- 6.1 Introduction
- 6.2 Theory of Dielectrics
 - 6.2.1 Brief Description of dielectrics
 - 6.2.2 The Debye theory of dielectrics
- 6.3 Experimental Details
- 6.4 Results and Discussion
- References

6.1 Introduction

The ac electrical properties of PPBMI thin films are discussed in this chapter. The ac conductivity and dielectric properties of PPBMI thin films have been discussed in the subsequent sections. This provides information regarding the conduction mechanism and dielectric properties of PPBMI thin films.

Because of good dielectric properties, plasma-polymerized thin films have been found to be useful as thin film insulators and capacitors in electrical and electronic devices like thin film dielectrics, separation membranes for batteries etc. As the materials have good dielectric properties, plasma polymerized thin films have been found to be useful as dielectrics in integrated microelectronics and insulating layers for semiconductors. Thin films produced through glow discharge are known to have free radicals or polar groups independent of the nature of monomers. Owing to this reason, these polymers are good candidates for the investigation of dielectric properties. A dielectric study throws light on the molecular structure and relaxation behaviors of the polymers.

The detail investigation of the ac conductivity and dielectric properties of plasma polymerized thin films provide information about the conduction process, dielectric constant, relaxation process etc which are dependent on frequency and temperature.

6.2 Theory of Dielectrics

6.2.1 Brief Description of dielectrics [1-6]

A dielectric is a nonconducting substance, i.e. an insulator. Although dielectric and insulator are generally considered synonymous, the term dielectric is more often used when considering the effect of alternating electric fields on the substance while insulator is more often used when the material is being used to withstand a high electric field. Dielectric materials can be solids, liquids, or gases. In addition, a high vacuum can also be a useful, lossless dielectric even though its relative dielectric constant is only unity. Solid dielectrics are perhaps the most commonly used dielectrics in electrical engineering, and many solids are very good insulators for example porcelain, parylene, glass, and plastics, mineral oil, piezoelectric material, ferroelectric materials etc. Air, nitrogen and sulfur hexafluoride are the three most commonly used gaseous dielectrics. If a material contains polar molecules, they will generally be in random orientations when no electric field is applied. An applied electric field will polarize the material by orienting

the dipole moments of polar molecules. This decreases the effective electric field between the plates and will increase the capacitance of the parallel plate structure

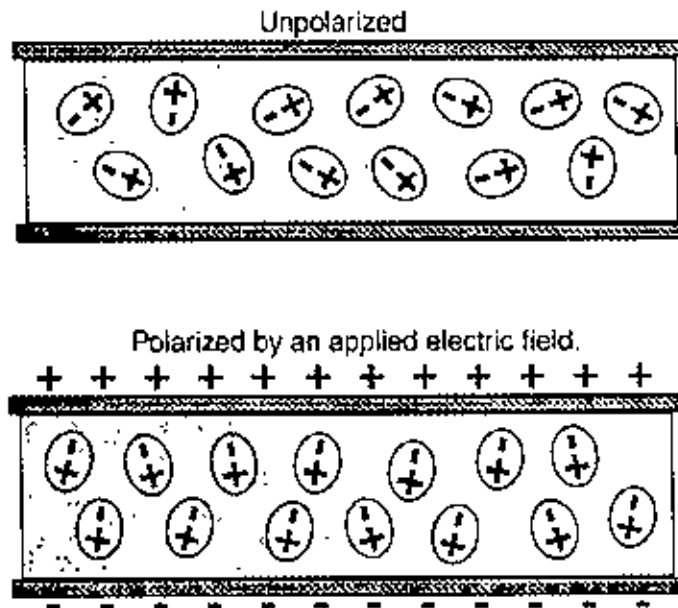


Fig 6.1 Polarization of dielectrics

One important property of a dielectric material is its permittivity. Permittivity (ϵ) is a measure of the ability of a material to be polarized by an electric field. The dielectric constant (k) of a material is the ratio of its permittivity ϵ to the permittivity of vacuum ϵ_0 , so $k = \epsilon / \epsilon_0$. The dielectric constant is therefore also known as the relative permittivity of the material. The dielectric constant of vacuum is one. Any material is able to polarize more than vacuum, so the k of a material is always greater than one. The dielectric constant is also a function of frequency in some materials, e.g., polymers, primarily because polarization is affected by frequency. A low- k dielectric is a dielectric that has a low permittivity, or low ability to polarize and hold charge. Low- k dielectrics are very good insulators for isolating signal-carrying conductors from each other. A high- k dielectric, on the other hand, has a high permittivity. Because high- k dielectrics are good at holding charge, they are the preferred dielectric for capacitors. High- k dielectrics are also used in memory cells that store digital data in the form of charge. Dielectric losses result from the heating effect on the dielectric material between the conductors. Power from the source is used in heating the dielectric. The heat produced is dissipated into the surrounding medium. When there is no potential difference between

two conductors, the atoms in the dielectric material between them are normal and the orbits of the electrons are circular. When there is a potential difference between two conductors, the orbits of the electrons change. The excessive negative charge on one conductor repels electrons on the dielectric toward the positive conductor and thus distorts the orbits of the electrons. A change in the path of electrons requires more energy, introducing a power loss.

6.2.2 The Debye theory of dielectrics

The capacitance of a parallel plate capacitor having a dielectric medium is expressed as

$$C = \frac{\epsilon_0 \epsilon' A}{d} \dots\dots\dots(6.1)$$

where ϵ_0 is the permittivity of free space, ϵ' is the dielectric constant of the medium, A is the surface area of each of the plates/electrodes and d is the thickness of the dielectric.

A real capacitor can be represented with a capacitor and a resistor. The parameters such as angular frequency (ω) of the applied field, the parallel resistance R_p , parallel capacitance C_p and the series resistance R_s and series capacitance C_s are related to the dielectric constant ϵ' , dielectric dissipation factor ϵ'' and loss tangent as:

$$\epsilon' = \frac{C_p}{C_0} \dots\dots\dots(6.2)$$

$$\epsilon'' = \frac{1}{R_p C_0 \omega} \dots\dots\dots(6.3)$$

and

$$\tan \delta = \frac{\epsilon''}{\epsilon'} = \frac{1}{R_p C_p \omega} = \frac{G_p}{2\pi f C_p} \dots\dots\dots(6.4)$$

The ac conductivity of σ_{ac} , was calculated using equation

$$\sigma_{ac} = G_p d / A \dots\dots\dots(6.5)$$

The dependence of ac conductivity, σ_{ac} , on frequency may be described by the power law [7]:

$$\sigma_{ac}(\omega) = A \omega^n \dots\dots\dots(6.6)$$

where A is a proportionality constant and ω ($=2\pi f$, f is the linear frequency) is the angular frequency and n is the exponent, which generally takes the value less than unity

for Debye type mechanism and is used to understand the conduction / relaxation mechanism in amorphous materials.

The dielectric behavior of a material is usually described by Debye dispersion equation [8]:

$$\epsilon^*(\omega, T) = \epsilon' - i\epsilon'' \dots\dots\dots(6.7)$$

where ϵ^* is the complex dielectric permittivity, ϵ' (energy dissipated per cycle) is the real part of complex dielectric permittivity and ϵ'' (energy stored per cycle) is the imaginary part of the complex dielectric permittivity.

$$\epsilon' = \epsilon_\infty + \frac{\epsilon_0 - \epsilon_\infty}{1 + \omega^2\tau^2} \dots\dots\dots(6.8)$$

$$\epsilon'' = \frac{(\epsilon_0 - \epsilon_\infty)\omega\tau}{1 + \omega^2\tau^2} \dots\dots\dots(6.9)$$

where ϵ_0 is the static or relaxed dielectric constant at ($\omega = 0$), ϵ_∞ is the high frequency or unrelated dielectric constant and the quantity τ is a characteristic time constant, usually called the dielectric relaxation time, it refers to a gradual change in the polarization following an abrupt change in applied field.

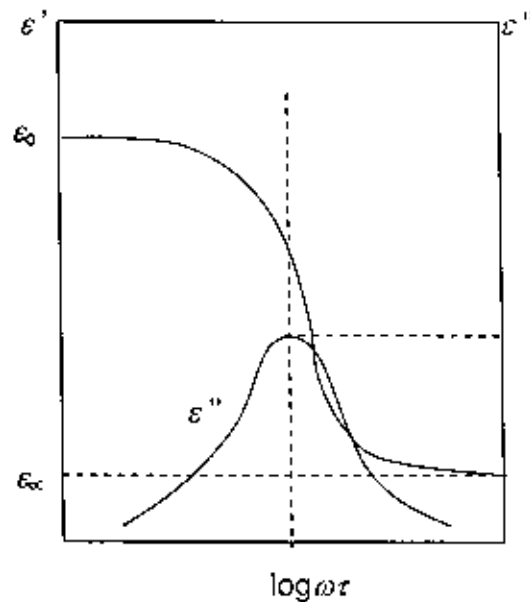


Fig 6.2 Debye dielectric dispersion curves.

The dielectric loss tangent is expressed by

$$\tan \delta = \frac{\epsilon''}{\epsilon'} \quad (6.10)$$

The graphs of ϵ' and ϵ'' against frequency of the applied field (logarithmic scale) through the dispersion regions show that the maximum loss value occurs when $\omega\tau = 1$, corresponding to a critical frequency $\omega_{\max} = 1/\tau$, and location of this peak provides the easiest way of obtaining the relaxation time from the experimental results.

6.3 Experimental Details

Sample preparation

The Al/PPBMI/Al sandwich structure samples were prepared for ac measurements. The thicknesses of the thin films for ac measurements are 150 nm and 200 nm.

Contact Electrodes for Electrical Measurements

Electrode Material

Aluminium (Al) (purity of 4N British Chemical Standard) was used for electrode deposition. Al has been reported to have good adhesion with glass slides, Al film has advantage of easy self-healing burn out of flaws in sandwich structure [9].

Electrode Deposition

Electrodes were deposited using an Edward coating unit E-306A (Edward, UK). The system was evacuated by an oil diffusion pump backed by an oil rotary pump. The chamber could be evacuated to a pressure less than 10^{-5} torr. The glass substrates were masked with 0.08 m X 0.08 m X 0.001 m engraved brass sheet for the electrode deposition. The electrode assembly used in the study is shown in Fig 6.4

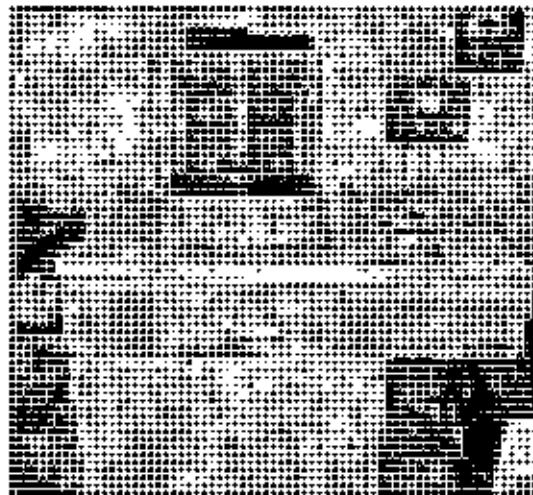


Fig 6.3 The Edward vacuum coating unit E306A.

The glass substrates with mask were supported by a metal rod 0.1 m above the tungsten filament. For the electrode deposition Al was kept on the tungsten filament. The filament was heated by low-tension power supply of the coating unit. The low-tension power supply was able to produce 100 A current at a potential drop of 10 V. During evacuation of the chamber by diffusion pump, the diffusion unit was cooled by the flow of chilled water and its outlet temperature was not allowed to rise above 305 K. When the penning gauge reads about 10^{-5} Torr, the Al on tungsten filament was heated by low-tension power supply unit it was melted.

The Al was evaporated, thus lower electrode onto the glass slide was deposited. Al coated glass substrates were taken out from the vacuum coating unit and were placed on the middle of the lower electrode of the plasma deposition chamber for PPBMI thin film deposition under optimum condition. The top Al electrode was also prepared on PPBMI thin film.

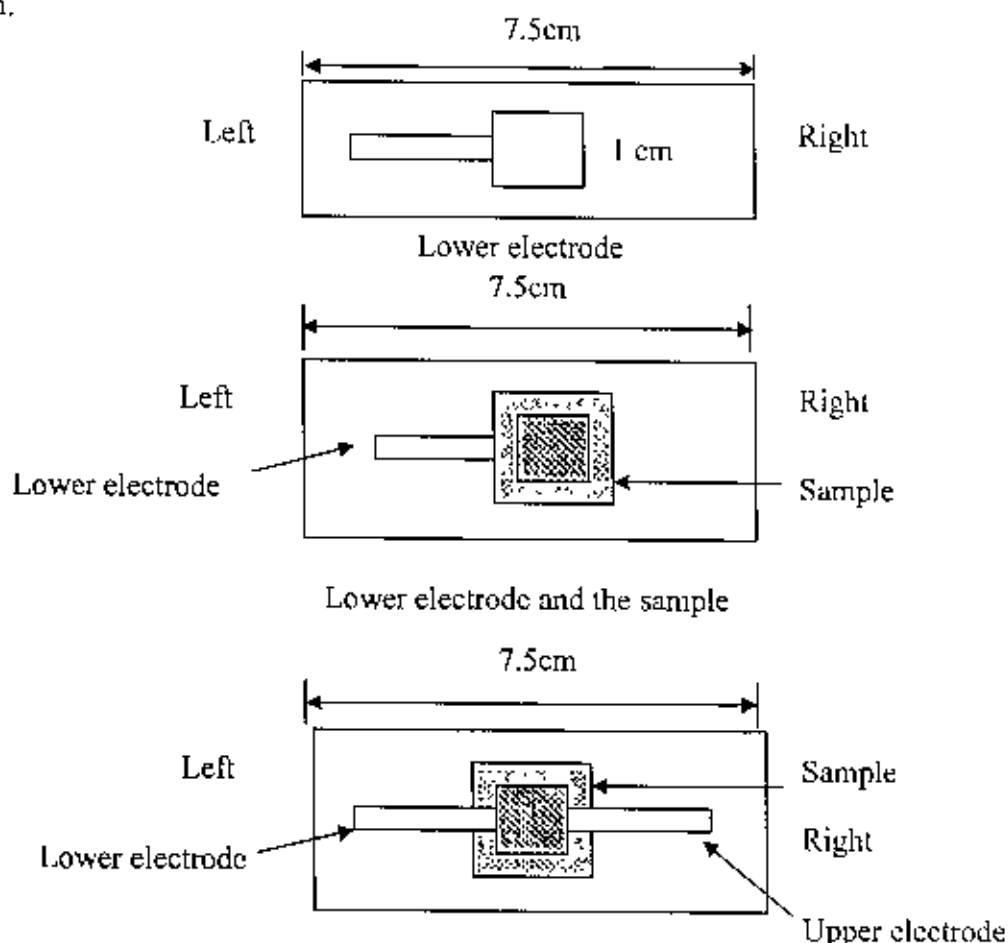


Fig 6.4 The electrode assembly

Measurement of dielectric properties by an Impedance Analyzer

The ac measurement was performed in the frequency range from 10^1 to 10^6 Hz and temperature range 298 – 398 K, by a low frequency (L.F) Impedance analyzer, Agilent 4192A, 5Hz-13MHz, Agilent Technologies Japan, Ltd. Made in Japan.

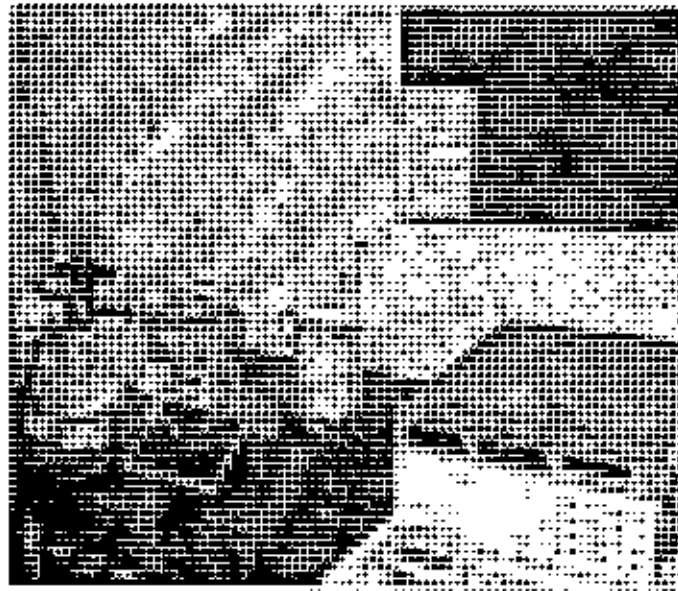


Fig 6.5 Photographs of the ac electrical measurement set-up.

The temperature was recorded by a Chromel-Alumel thermocouple placed very close to the sample which was connected to a Keithley 197A digital microvoltmeter. To avoid oxidation, all measurements were performed in a vacuum of about 10^{-2} Torr. Photographs of the Impedance analyzer and ac measurement set-up are shown in Fig 6.5.

6.4 Results and Discussion

6.4.1 Variation of ac conductivity with frequency and temperature

The dependence of ac conductivity on frequency at different temperature of PPBMI thin films is shown in Fig 6.6. From the figure it is revealed that the conductivity of the thin

films increases linearly with frequency. The dependence of ac conductivity on frequency

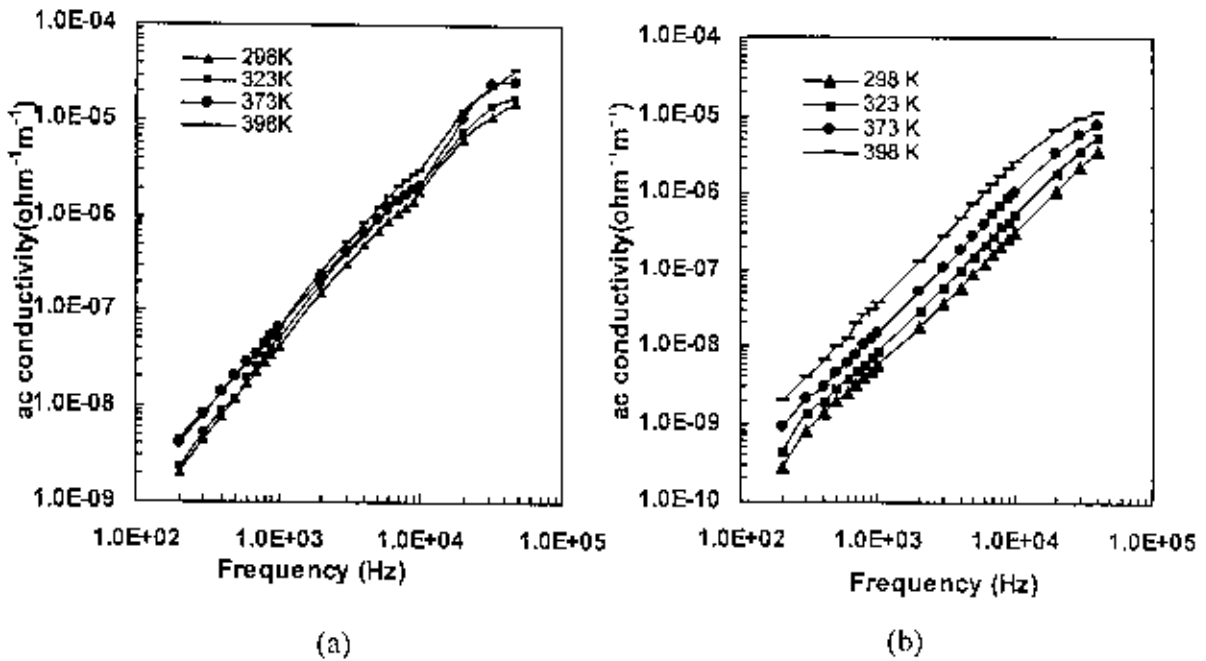


Fig 6.6 Conductivity versus frequency of the PPBMI thin films of thicknesses (a) 150 nm and (b) 200 nm at different temperatures.

follows the power law $\sigma_{ac}(\omega) = A\omega^n$, where $n < 1$ for Debye type mechanism and $n > 1$ for other mechanisms. The values of the exponent 'n' for PPBMI thin films are found to be 1.50 to 1.87 which are depicted in Table 6.1. These suggest that the Debye type of loss mechanism is not operative in this materials.

Table 6.1 Values of 'n' at different measurement temperatures of PPBMI thin films of various thicknesses.

Sample Thickness (nm)	Measurement Temperature (K)	Values of 'n'
150	298	1.64
	323	1.61
	373	1.50
	398	1.64
200	298	1.81
	323	1.80
	373	1.87
	398	1.82

The variation of ac conductivity with temperature is plotted in Fig 6.7 using the equation $\sigma_{ac} = \sigma_0 e^{-1/KT}$. The value of ac conductivity increases slowly at low temperature. Activation energies from these curves have been calculated and is recorded in Table 6.2.

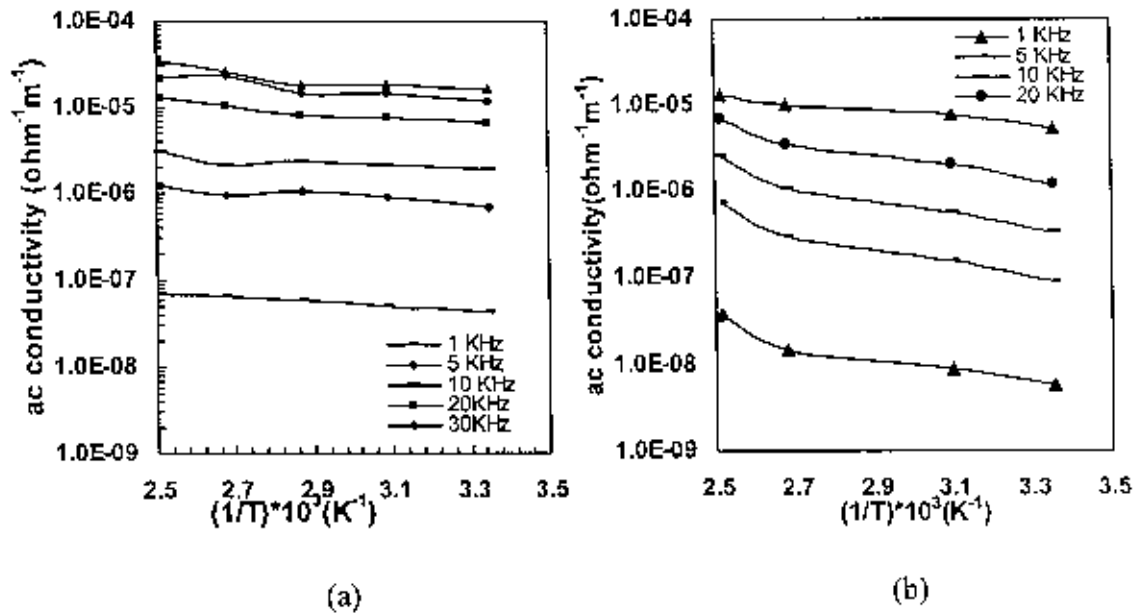


Fig 6.7 Conductivity versus temperature of the PPBMI thin films of thicknesses (a) 150 nm and (b) 200 nm at different frequencies.

These are found to be 0.05 to 0.13 eV. These small values of activation energy indicate hopping type of conduction mechanism in the PPBMI thin films due to motion of the carriers within the defect states present in the band tails of the PPBMI thin films.

Table 6.2 Values of 'activation energy' at different frequency for PPBMI thin films of different thicknesses

Thickness (nm)	Frequency (kHz)	Activation Energy (eV)
150	1 kHz	0.05
	20 kHz	0.06
	40 kHz	0.07
200	1 kHz	0.10
	10 kHz	0.13
	20 kHz	0.12
	50 kHz	0.06

6.4.2 Variation of dielectric constant with frequency and temperature

The change of dielectric constant with frequency and temperature of PPBMI thin films is shown in Fig 6.8 and Fig 6.9 respectively. The ϵ' decreases with increasing frequency.

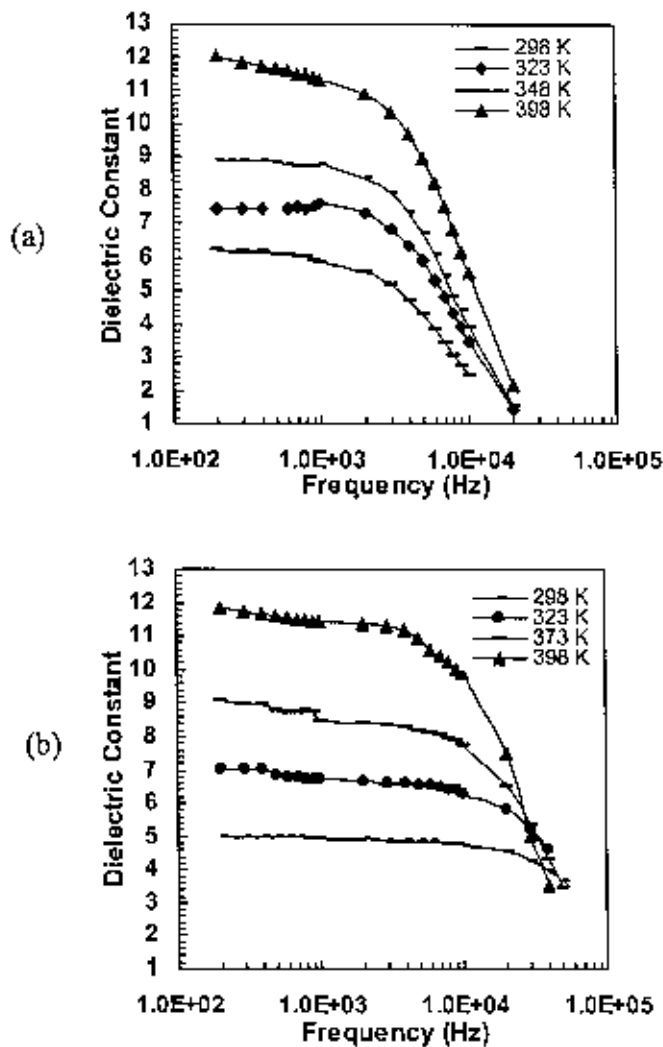


Fig 6.8 Dielectric Constant versus frequency of the PPBMI films of Thicknesses (a) 150 nm and (b) 200 nm at different temperatures.

But this decreasing rate is less at the low frequency region and higher at the high frequency ($>10^4$ Hz) region. The rapid decrease of ϵ' around 10^4 Hz may be due to non-response of the polarizing species in PPBMI thin films.

It is revealed that the dielectric constant of the thin films increases with increasing temperature and it is found to be 5 to 12 for 298 to 398 K at low frequency. It is also revealed that the ϵ' of the material does not depend significantly on thickness of the PPBMI thin films.

The dependence of dielectric constant with temperature of PPBMI thin films is shown in Fig 6.9. From the figure it is revealed that the rate of increase of ϵ' is less in the low

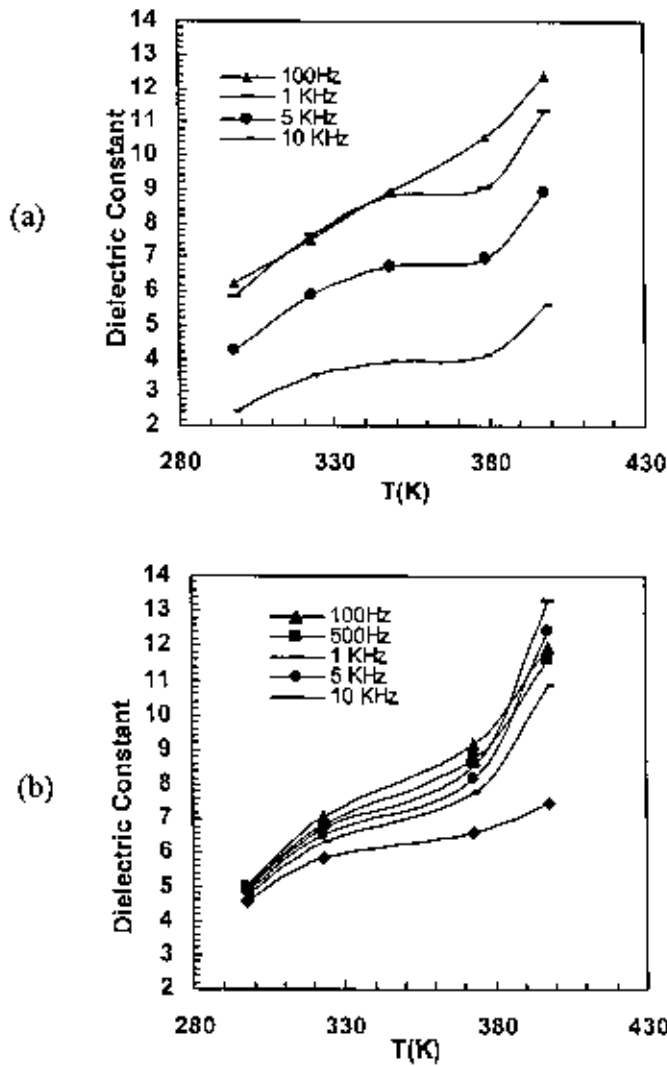


Fig 6.9 Dielectric Constant as a function of temperature of the PPBMI thin films of thicknesses (a) 150 nm and (b) 200 nm at different frequencies.

temperature region and higher in the high temperature (>380 K) region. There are reports of thickness dependence of dielectric constant of plasma polymerized 1,1,3,3 - Tetramethoxypropane thin films [11]. It is to be mentioned here that the optical band gap of this thin film is also not significantly dependent on thickness. This supports the independency of dielectric constant with thickness of this material.

6.4.3 Variation of dielectric loss tangent with frequency and temperature

The Fig 6.10 shows the variation of dielectric loss tangent with frequency at different temperature. It shows that the dielectric loss of the thin films increases exponentially with frequency.

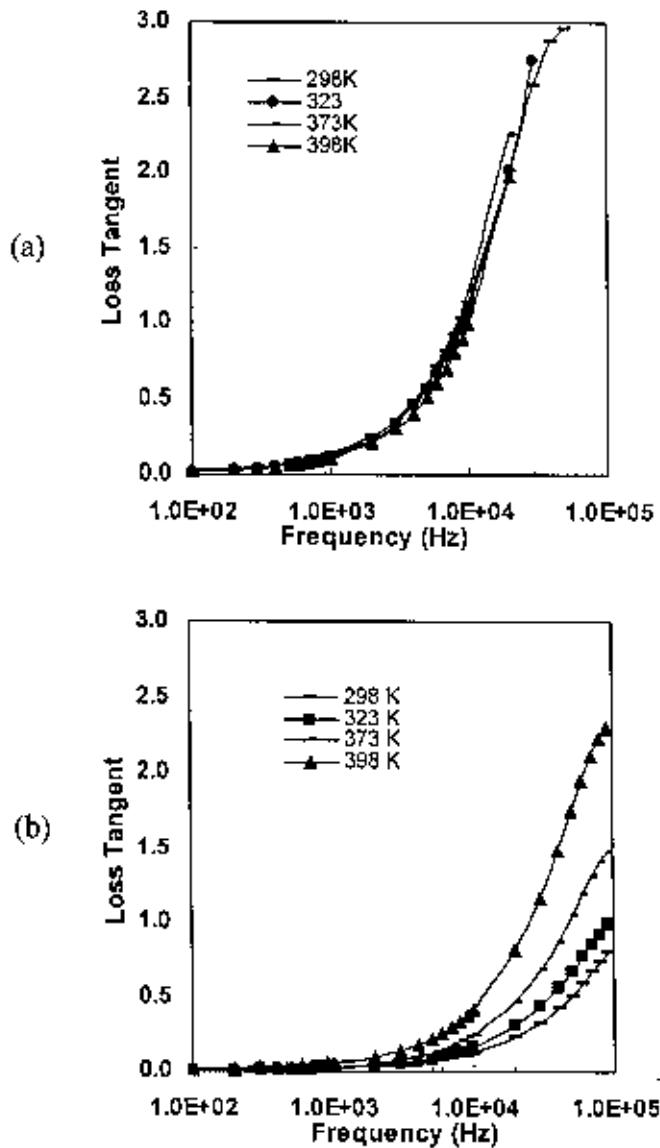


Fig 6.10 Loss Tangent versus frequency of the PPBMI thin films of thicknesses (a) 150 nm and (b) 200 nm at different temperatures.

The dependence of dielectric loss tangent with temperature at different frequencies is plotted in Fig 6.11. From the figure, it is revealed that the loss tangent of the material increases with increasing temperature. The dielectric losses increases slowly at the low temperature region (<380 K) and increases rapidly at the higher temperature (>380 K).

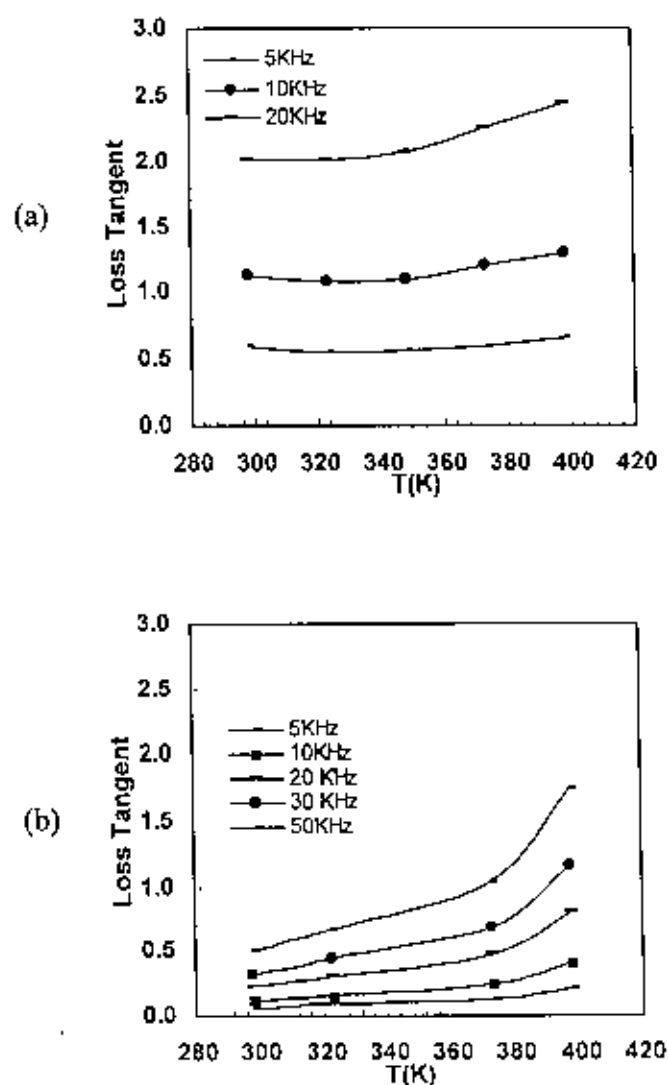


Fig 6.11 Loss Tangent as a function of temperature of the PPBMI thin films of thicknesses (a) 150 nm and (b) 200 nm at different frequencies.

It is observed that the loss peak may occur at higher frequency and higher temperature. The high loss value at the high frequency and temperature may be due to the presence of carbonyl group in the sample. The presence of oxygen in the sample recorded by FTIR analysis supports this fact.

References

- [1] http://en.wikipedia.org/wiki/cite_note-1#cite_note-1.
- [2] http://en.wikipedia.org/wiki/cite_note-2#cite_note-2.
- [3] Daintith, "Biographical encyclopedia of scientists", CRC Press, (1994) 943.
- [4] Von Hippel A. R., "Dielectric materials and applications", Technology Press of MIT and John Wiley, NY (1954).
- [5] Sarma P. and Hylten-Cavallius N., "Capacitance calculations for some basic high voltage electrode configurations", IEEE Transactions on Power Apparatus and Systems 94 5 (1975) 1708-1713.
- [6] Ramo S., Whinnery J.R., and Van Duzer T., "Fields and waves in communication electronics", John Wiley and Sons, NY (1994).
- [7] Davis E. A. and Mott N. F., "Electronic processes in non-crystalline materials", Clarendon Press, Oxford (1971).
- [8] Blythe A. R., "Electrical properties of polymers", Cambridge University Press, Cambridge (1979) 69-71.
- [9] Lamb D. R., "Electrical conduction mechanisms in thin insulating films", Methuen and Co. Ltd., London (1967).
- [10] Shah Jalal A. B. M., Ahmed S., Bhuiyan A. H. and Ibrahim M., "On the conduction mechanism, in plasma polymerized m-Xylene thin films", Thin Solid Films 288 (1996) 108-111.
- [11] Tamanna Afroze, "Investigation of the dielectric relaxation in plasma polymerized 1,1,3,3 Tetramethoxypropane thin films", M.Phil. Thesis, BUET, Dhaka (2007).

CHAPTER VII

CONCLUSIONS

- 7.1 Conclusions
- 7.2 Suggestions for Further Work

7.1 Conclusions

The PBMI thin films were prepared by plasma polymerization technique using a capacitively couple reactor. The structural, optical and ac electrical properties of PPBMI thin films were studied. Based on the results and discussion the following conclusions can be drawn.

The SEM investigation reveals that the PPBMI thin film deposited on to glass substrates are smooth, uniform and pinhole free. FTIR investigation shows that the chemical structure of PPBMI thin films is different from that of BMI monomer. This observation reveals that the PPBMI thin films may contain conjugation in the aromatic structure, C=O and OH groups. The conjugation proceeds through abstraction of hydrogen from the BMI spectra owing to plasma polymerization. The oxygen incorporated from the atmosphere when the BMI was exposed to atmosphere.

UV-Vis absorption spectra show a red shift for all PPBMI thin films as compared to the monomer, which indicates the presence of certain amount of conjugation. Both allowed direct (E_{qd}) and indirect (E_{qi}) transitions were identified in PPBMI thin films. The E_{qd} is about 3.00 eV and E_{qi} is about 2.0 eV. The calculated value of Tauc parameter, B, is $260 \text{ (cm)}^{-1/2} \text{ (eV)}^{-1/2}$. The dependence of k on photon energy indicated that the probability of electron transfer across the mobility gap rises with the photon energy.

The ac conductivity of PPBMI thin films increases linearly with frequency. The dependence of ac conductivity on frequency follows the power law $\sigma_{ac}(\omega) = A\omega^n$, where $n < 1$ for Debye type mechanism and $n > 1$ for other mechanisms. These suggest that the Debye type of loss mechanism is not operative in these materials.

The ac conductivity increases slowly at low temperature. Activation energies are found to be 0.05 to 0.13 eV. These small values of activation energy indicate hopping type of conduction mechanism in the PPBMI thin films.

The ϵ' decreases with increasing frequency. But this decreasing rate is less at the low frequency region and higher at the high frequency ($>10^4$ Hz) region. The rapid decrease of ϵ' around 10^4 Hz may be due to non-response of the polarizing species in PPBMI thin films. It is revealed that the dielectric constant of PPBMI thin films increase with increasing temperature and it is found to be 5 to 12 for 298 to 398 K. It is also revealed

that the ϵ' of PPBMI thin films does not depend significantly on thickness of the films for the film thicknesses used in this investigation.

It is seen that value of dielectric loss increases with increasing frequency and temperature. The loss peak may occur at the higher frequency and higher temperature. The high loss value at the high frequency and temperature may be due to the presence of C=O in the samples. The presence of oxygen in the sample recorded by FTIR analysis supports this fact.

Finally it can be inferred that the optical and electrical property of PPBMI thin films is not significantly dependent on thickness for the PPBMI thickness up to 200 nm. This signifies that PPBMI thin films are uniform through the bulk.

7.2 Suggestions for Further Work

The present work shows the investigation of the structural, optical and ac electrical behavior of PPBMI thin films. But more investigations on PPBMI thin films are required to know the different characteristics, which will help finding suitable applications of these materials. The following investigations may be carried out for further study.

The thermal analysis by differential scanning calorimetry (DSC), differential thermal analysis (DTA) and thermogravimetric analysis (TGA) at different heating rates will be helpful to ascertain the reaction kinetics in the PPBMI thin films. To observe the nature and source of radicals in PPBMI thin films, the electron spin resonance (ESR) study may be carried out.

DC electrical measurements can be carried out to find the J-V characteristics and conduction mechanism. For studying the charge storage and charge relaxation, the thermally stimulated depolarization current (TSDC) can be measured.


```
Call viOpen(defrm, "GPIB0::17::INSTR", 0, 0, vi)
```

```
Call viVPrintf(vi, "**RST" + Chr$(10), 0)
```

```
Call viVPrintf(vi, "**IDN?" + Chr$(10), 0)
```

```
Call viVScanf(vi, "%t", strRes)
```

```
'MsgBox "Result is: " + strRes, vbOKOnly, "**IDN? Result"
```

```
strResTrim = RTrim(strRes)
```

```
strRes1 = InStr(1, strResTrim, ",", 0)
```

```
strRes2 = Left(strResTrim, strRes1 - 1)
```

```
txtVar1.Text = Val(Mid(strRes2, 5))
```

```
strRes3 = Val(RTrim(Mid(strResTrim, strRes1 + 5)))
```

```
txtVar2.Text = strRes3
```

```
Call viClose(vi)
```

```
Call viClose(defrm)
```

```
End Sub
```

```
Private Sub cboFrequency_DropDown()
```

```
cboFrequency.Clear
```

```
Dim Counter As Long
```

```
Dim x1
```

```
If Counter = 0 Then
```

```
For x1 = 10 To 100 Step 10
```

```
cboFrequency.AddItem Str(x1)
```

```
Next x1
```

```
Counter = 100
```

```
End If
```

```
If Counter = 100 Then
```

```
For x1 = 200 To 900 Step 100
```

```
cboFrequency.AddItem Str(x1)
```

```
Next x1
```

```
Counter = 1000
```

```
End If
```

```
If Counter = 1000 Then
```

```
For x1 = 1 To 9 Step 1
```

```
cboFrequency.AddItem Str(x1) & "K"
```

```
Next x1
```

```
Counter = 10000
```

```
End If
```

```

If Counter = 10000 Then
  For x1 = 10 To 100 Step 10
    cboFrequency.AddItem Str(x1) & "K"
  Next x1
  Counter = 100000
End If
If Counter = 100000 Then
  For x1 = 200 To 900 Step 100
    cboFrequency.AddItem Str(x1) & "K"
  Next x1
  Counter = 1000000
End If
If Counter = 1000000 Then
  For x1 = 1 To 13 Step 1
    cboFrequency.AddItem Str(x1) & "M"
  Next x1
End If
End Sub

Private Sub cmdAddToDatabase_Click()

  On Error Resume Next

  If Right(cboFrequency.Text, 1) = "K" Then
    cboFrequency.Text = Val(cboFrequency.Text) * 1000
  ElseIf Right(cboFrequency.Text, 1) = "M" Then
    cboFrequency.Text = Val(cboFrequency.Text) * 1000000
  End If

  Data1.Recordset.AddNew

  cboFrequency.Enabled = True
  cboFrequency.SetFocus
End Sub
Private Sub cmdClear_Click()
  cboFrequency.Text = ""
  txtVar1.Text = ""
  txtVar2.Text = ""
End Sub

Private Sub cmdClose_Click()
  Unload Me
End Sub

Private Sub cmdDelete_Click()
  If Data1.Recordset.RecordCount = 0 Then

```

```
    MsgBox "There is no record!"
    cmdAddToDatabase.SetFocus
    Exit Sub
End If
Dim confirm
confirm = MsgBox("Are you sure?", vbYesNo + vbQuestion, "Delete")
If confirm = vbYes Then
    Data1.Recordset.Delete
    Data1.Recordset.MoveNext
    If Data1.Recordset.RecordCount = 0 Then
        cboFrequency.Enabled = False
    End If
End If
End Sub

Private Sub cmdEdit_Click()
    Data1.Recordset.Edit
End Sub

Private Sub cmdFirst_Click()
    On Error Resume Next
    If Data1.Recordset.RecordCount = 0 Then
        MsgBox "There is no record!"
        cmdAddToDatabase.SetFocus
        Exit Sub
    End If
    Data1.Recordset.MoveFirst
End Sub

Private Sub cmdLast_Click()
    On Error Resume Next
    If Data1.Recordset.RecordCount = 0 Then
        MsgBox "There is no record!"
        cmdAddToDatabase.SetFocus
        Exit Sub
    End If
    Data1.Recordset.MoveLast
End Sub

Private Sub cmdNext_Click()
    On Error Resume Next
    If Data1.Recordset.RecordCount = 0 Then
        MsgBox "There is no record!"
        cmdAddToDatabase.SetFocus
        Exit Sub
    End If
End Sub
```


End If

```
Data1.Recordset.MoveNext
If Data1.Recordset.EOF = True Then
    MsgBox "This is last record!"
    Data1.Recordset.MoveLast
End If
```

End Sub

```
Private Sub cmdPrevious_Click()
    On Error Resume Next
    If Data1.Recordset.RecordCount = 0 Then
        MsgBox "There is no record!"
        cmdAddToDatabase.SetFocus
        Exit Sub
    End If
```

```
Data1.Recordset.MovePrevious
If Data1.Recordset.BOF = True Then
    MsgBox "This is first record!"
    Data1.Recordset.MoveFirst
End If
```

End Sub

```
Private Sub cmdRead_Click()
```

```
    Main
```

```
End Sub
```

```
Private Sub cmdReSet_Click()
```

```
    Dim reset As Integer
```

```
    Dim x
```

```
If cboFrequency.Text = "" Then
    cmdAddToDatabase.SetFocus
    Exit Sub
End If
```

```
Data1.Recordset.MoveLast
reset = Data1.Recordset.RecordCount
x = 1
```

```
If reset = 0 Then
    cmdAddToDatabase.SetFocus
    Exit Sub
```

```
Else
```

```
    Do While x <= reset
        Data1.Recordset.MoveFirst
        Data1.Recordset.Delete
```

```
Data1.Recordset.MoveNext  
x = x + 1  
Data1.Refresh  
.Loop  
cmdAddToDatabase.SetFocus  
End If
```

End Sub

```
Private Sub cmdSearch_Click()  
Dim search  
search = InputBox("Enter a Frequency:")  
Data1.RecordSource = "Select * from VisaProgram Where Frequency =" &  
Val(search) & ""  
Data1.Refresh  
End Sub
```

```
Private Sub cmdShowAll_Click()  
Data1.RecordSource = "Select * from VisaProgram"  
Data1.Refresh  
End Sub
```

```
Private Sub Form_Load()  
Me.Height = 6000  
Me.Width = 10500  
End Sub
```

